



POLITECNICO
MILANO 1863

SCUOLA DI INGEGNERIA INDUSTRIALE
E DELL'INFORMAZIONE

Optimal Design of Multiple-Effect Evaporation for Tomato Paste: A Techno-Economic Approach Supported by Digital Twin Simulation

TESI DI LAUREA MAGISTRALE IN
FOOD ENGINEERING

Gaia Lunari, 247017
Silvia Serena Mariani, 247068

Advisor:
Prof. Flavio Manenti

Co-advisors:
Ing. Marcello Maria Bozzini

Academic year:
2024-2025

Abstract: This thesis examines the design, optimization, and dynamic simulation of a forward-feed multiple-effect evaporation system for tomato paste production. Tomato paste (30 °Brix), obtained from tomato juice (5 °Brix) concentration, and rich in bioactive compounds such as lycopene, pectin, and vitamin C, is a globally relevant food ingredient whose quality depends on processing conditions. The study combines the design of the system and cost analysis to determine the optimal number of effects for the evaporation process, and applies Industry 4.0 Digital Twin technology to simulate its dynamic behavior. Thanks to a comparative economic evaluation of configurations with one to five effects considering capital expenditures, operating expenditures, and total costs over the plant's lifetime, a three-effect forward-feed configuration offers the lowest total cost. A Digital Twin of the optimal configuration, developed in AVEVA Dynamic Simulation software, reproduces the system's dynamic behavior and enables simulations of start-up and shutdown operations. The model demonstrates reliable process control, stable start-up performance, and safe vessel drainage during shutdown. Overall, the work shows how Digital Twins enhance process understanding, operational safety, and decision-making in the food industry, while promoting sustainability and competitiveness.

Key-words: tomato paste production, multiple-effect evaporation, digital twin, process optimization, cost analysis, food engineering

1. Introduction

Tomatoes are widely used across a broad range of processed food products thanks to their appealing taste, vibrant color, and functional consistency. Figure 2 illustrates that from fresh tomatoes, various items can be produced, including dehydrated tomatoes, tomato pulp, ketchup, tomato paste, tomato powder, tomato juice, chili sauce, and canned tomatoes. Among these, some of the most commonly consumed processed tomato products are juice, sauce, paste, ketchup, soup, and canned tomatoes. This diversity in tomato processing reflects its significant role in the food industry and the broad range of culinary applications.

The global tomato processing market was valued at approximately USD 51.8 billion in 2023, with tomato paste and purees accounting for about USD 8.2 billion, highlighting their significant role within the broader processed food sector [7]. In 2024, global tomato paste production reached a record 45.8 million tons (Figure 1), surpassing

the 44.4 million tons produced the previous year. This growth reflects increasing demand and underscores tomato paste’s critical importance in the food industry [11].

Major producers include China, the United States, Italy, Spain, and Turkey, which together supply this growing global demand. Exports have also surged, reaching a record 3.8 million tons in one year [8], reflecting tomato paste’s widespread acceptance and integration into global food markets. Given this industrial and economic significance, optimizing tomato processing is essential for improving quality, sustainability, and market competitiveness.

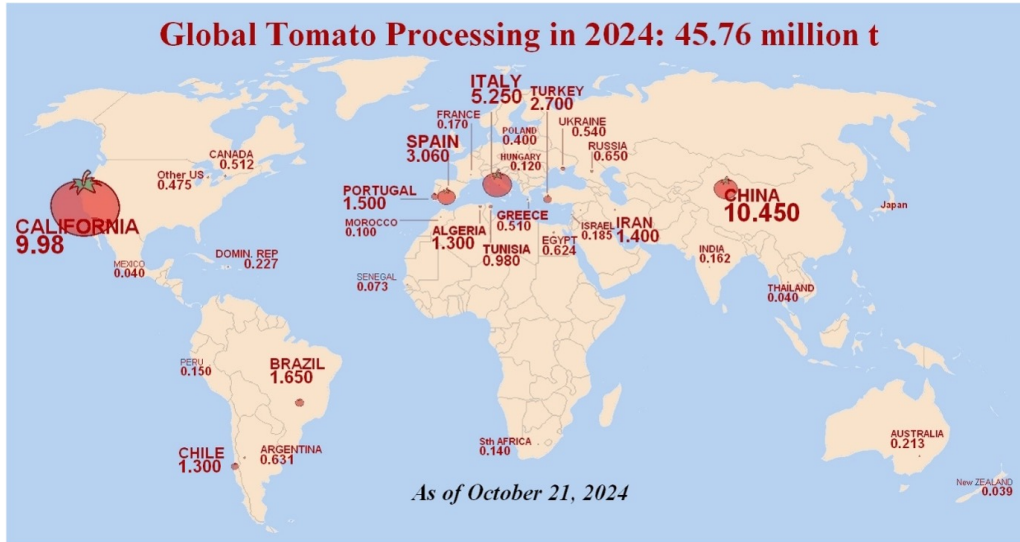


Figure 1: Global Tomato Processing of 2024 [39]

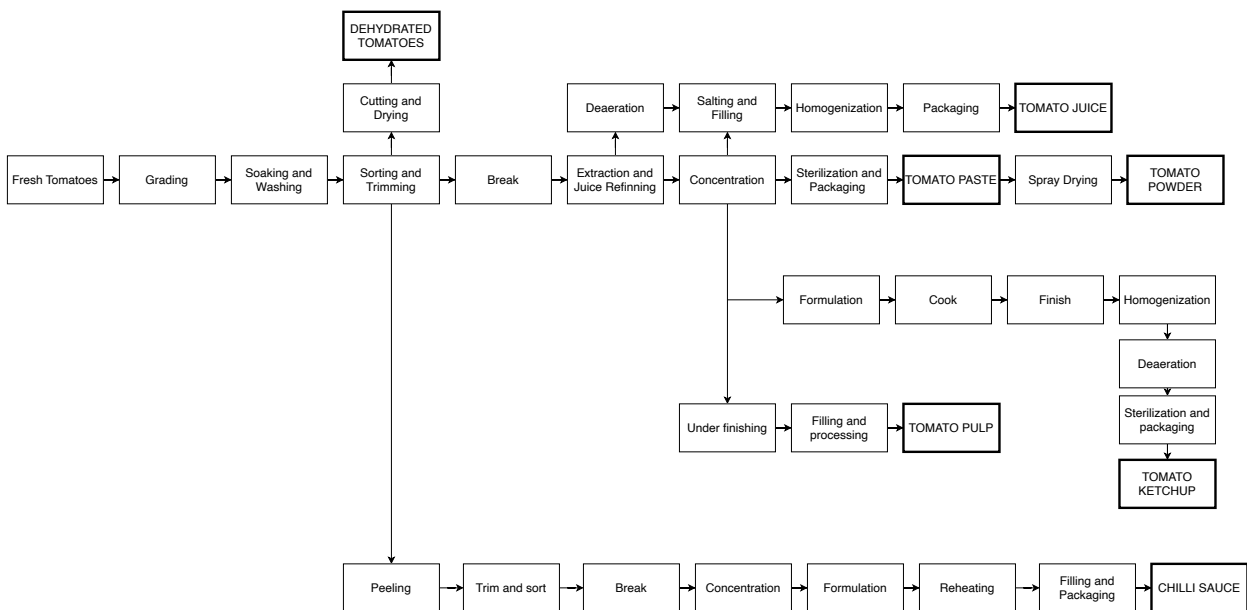


Figure 2: Process flow diagram of tomato products [4]

This thesis focuses specifically on the production and processing of tomato paste. Tomato paste, a concentrated derivative of tomatoes, is a fundamental ingredient in global cuisines, forming the base for sauces, soups, and various culinary preparations. Its extended shelf life and rich flavor make it essential in both household kitchens and the food processing industry.

To fully understand the quality of tomato paste and the factors that influence it, it is essential to examine the processing steps involved in its production.

The processing of tomatoes involves several critical steps, each of which contributes to the quality of the final product. These steps, illustrated in Figure 3 must be carefully controlled to maintain product consistency,

flavor, and nutritional value.

Tomato paste production main step is evaporation to obtain a concentrated final product. Before performing this, a series of pretreatments are necessary, crucial for ensuring that the raw material is suitable for further transformation.

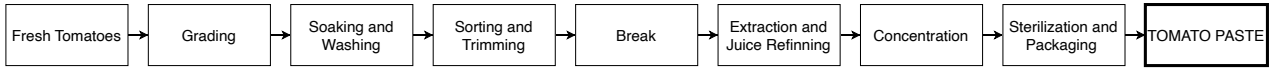


Figure 3: Process flow diagram of tomato paste

The first step is grading, which ensures that only tomatoes of the appropriate quality and ripeness level are used. Grading standards vary by country or company, and tomatoes are usually inspected based on defects such as worm damage, mold, and mechanical damage, and their color is visually evaluated. Tomatoes are categorized into different ripeness stages, from green to red, with each stage affecting the processing method [35].

Once the tomatoes are graded, they are washed to remove any dirt, debris, or microbial contamination. Washing typically involves two phases: soaking and spray-rinsing. The tomatoes are soaked in water, sometimes using high-pressure water jets, and then rinsed with fresh water. To control microbial populations, chlorine is often added to the wash water [4].

After washing, the tomatoes are sorted and trimmed to remove any defective fruit or parts. This can be done using roller conveyors and photoelectric sorters. This step ensures that only the highest-quality fruit is processed, with any under-ripe or defective tomatoes being discarded or repurposed for other products [4]. After sorting, the processing continues with coring, which aims to improve the final product's texture. This can be done by machine or by hand. Modern tomato varieties often have smaller cores, making this step less necessary [4].

Then the tomatoes are chopped in a process known as breaking, which can be done using either a hot-break or cold-break method. In hot-break processing, tomatoes are quickly heated to 82-93°C to deactivate pectolytic enzymes, which, if left active, can degrade pectin, a structural polysaccharide responsible for the texture and thickness of the final product. Preserving pectin and hemicelluloses during processing is crucial for obtaining a high-viscosity paste, especially when the raw material is naturally rich in these hydrocolloids. This results in a thicker, more stable product suitable for sauces and ketchup.

In cold-break processing, tomatoes are chopped at lower temperatures of 60-66°C, which results in a product with a more delicate flavor and color but lower viscosity, making it more suitable for applications where those characteristics are prioritized [14].

Following the break process, the pulp undergoes extraction and refining, which removes seeds, skins, and other impurities. This is typically done using screw-type or paddle-type extractors, which press or beat the pulp to extract juice. To minimize oxidation, which can degrade nutrients like lycopene and ascorbic acid, air incorporation is minimized during extraction [33].

Finally, the juice undergoes concentration, where its solids content is increased to produce a paste with the desired consistency. This is typically done using vacuum evaporators, which gradually increase the temperature and concentrate the juice to 24-38% solids [5]. For final packaging, the paste is hot-filled at a minimum of 90°C into cans, sealed without additional heat treatment, cooled after a water spray rinse, and finally packed [23].

Beyond their culinary attributes, tomatoes are also valued for their rich content of bioactive compounds, notably carotenoids such as lycopene, which is recognized for its antioxidant and anti-inflammatory properties, and its potential role in supporting cardiovascular and prostate health. Achieving high product quality largely depends on processing conditions, which affect key attributes such as viscosity, flavor retention, nutritional value, and lycopene bioavailability [40].

Among the various constituents that influence tomato sauce quality, three bioactive compounds play a particularly significant role in terms of their functional and nutritional relevance:

- **Lycopene**, a carotenoid responsible for the deep red color of tomatoes, significantly impacts both the visual appeal and the antioxidant properties of the sauce. It consists of a long-chain hydrocarbon structure with alternating single and double bonds, forming a conjugated system that absorbs light efficiently. Higher lycopene content generally indicates a richer color and greater nutritional value, making it an essential marker of tomato sauce quality. Lycopene exhibits notable stability during initial thermal treatments, such as the "hot break" process at 93°C for 5 minutes. However, further processing, including multi-stage evaporation and sterilization, can lead to a reduction of about 20% in lycopene content. To preserve lycopene during the evaporation stages, it is crucial to minimize oxygen exposure and optimize processing conditions [2].
- **Pectin**, a polysaccharide composed mainly of galacturonic acid units, is a key factor in determining the consistency and texture of tomato sauce. It has a natural ability to form gels by trapping water, which

influences the sauce's viscosity and stability. The degree of pectin methyl-esterification affects the gelling properties, with higher pectin content resulting in a thicker and more structured sauce. Pectin degradation is influenced by processing conditions, particularly heating. Rapid heating of crushed tomatoes can minimize pectin breakdown, preserving the final product's viscosity. Shortening the time gap between crushing and heating is essential to retain pectin, making it a crucial parameter in the production process [31].

- **Ascorbic acid (vitamin C)** also plays a fundamental role in defining the nutritional and sensory profile of tomato-based products. It enhances freshness, acidity, and contributes to oxidative stability, prolonging the shelf life of the final product. Structurally, it is a small, water-soluble molecule with strong antioxidant properties, but it is highly thermolabile and sensitive to oxygen. During industrial processing, ascorbic acid undergoes significant degradation, particularly during the initial thermal treatment stages. Studies have shown that losses of up to 44.4% may occur during tomato paste production, especially in processes involving high heat and oxygen exposure [21]. To preserve vitamin C content, minimizing residence time at elevated temperatures and operating under reduced oxygen conditions, such as vacuum evaporation, are essential strategies [19].

While lycopene, ascorbic acid, and pectin are fundamental to the quality of tomato sauce, other factors such as sugar content, acidity, and processing techniques also contribute to its overall characteristics. The balance of these elements determines the final product's color, taste, texture, and nutritional value, all of which are essential for consumer preference and marketability. Understanding the interplay between these components allows for better control over tomato sauce formulation and optimization of its quality.

This work primarily focuses on the evaporation stage within the tomato paste production process, an essential unit operation in the food industry, widely employed for concentrating liquid food products. In tomato paste production, the primary objective of evaporation is to remove a significant portion of water, around 50%, to enhance product consistency and flavor while preserving sensory and nutritional quality. The process is typically carried out under vacuum to reduce thermal degradation and preserving delicate compounds [18]. Evaporators work by removing water as vapor through heat exchange. Steam is used as the heating medium, releasing its latent heat to the product before condensing. To enhance energy performance, multiple-effect evaporators are adopted. These systems link several units in series, each operating at progressively lower pressures. The vapor from one stage serves as the heating medium for the next, significantly reducing steam consumption [30]. In accordance with the literature on multiple-effect evaporation applied to tomato paste production, this study considers configurations with one to five effects. This choice reflects typical design and operational ranges found in both simulation and optimization studies on tomato processing [27], [29].

In multiple-effect evaporation systems, the arrangement of product and steam flow significantly influences energy efficiency, process control, and final product quality. Three primary flow configurations are used: equicurrent (forward feed), countercurrent (backward feed), and mixed flow. Each has distinct advantages and is selected based on the properties of the product being concentrated.

This study focuses on a forward-feed (equicurrent) configuration, where both the tomato paste and steam move in the same direction, starting from the first effect, which operates at the highest temperature and pressure. This method is particularly suitable for heat-sensitive products like tomato paste, as it minimizes thermal damage by gradually reducing the temperature as the product moves through successive effects.

Key advantages of equicurrent flow are [3], [26], [41]:

- **Minimized thermal stress:** since the product is subjected to progressively lower temperatures, heat-sensitive compounds are better preserved. As the tomato product advances through the effects, its soluble solids content steadily increases, achieving the desired concentration by the final stage.
- **Simplified pumping requirements:** the natural pressure gradient allows the product to flow without excessive mechanical pumping, reducing operational costs and equipment wear.
- **Energy efficiency:** the heat from the first effect is efficiently transferred to subsequent effects, improving overall energy utilization.

This thesis also includes a cost analysis of the multistage evaporation process. Conducting a detailed cost analysis is a fundamental step in process design, as it enables engineers and decision-makers to assess the economic feasibility of the system. This involves evaluating all costs associated with the process, both at the investment stage and during regular operation. These costs are generally divided into two main categories: Capital Expenditures (CapEx) and Operating Expenditures (OpEx) [12].

- **CapEx** includes long-term investments such as machinery, buildings, or infrastructure that are expected to improve productivity over time. These expenses are not fully counted as a cost in the year they are made. Instead, their value is gradually deducted over the years, according to the expected lifespan of the asset, through a process called depreciation. [12] [16].

- **OpEx**, on the other hand, includes the regular, ongoing costs required to keep a process running, such as energy, raw materials, maintenance, and labor. Unlike CapEx, these expenses are recorded entirely in the same financial year in which they occur.[12] [17].

Finding the right balance between CapEx and OpEx is essential when making process design decisions. A higher initial investment may lead to lower operating costs over time, or vice versa. In tomato paste production, for instance, increasing the number of evaporation effects reduces steam consumption, lowering OpEx, but also raises CapEx due to additional equipment. The total cost over the plant’s lifetime, obtained by summing CapEx and cumulative OpEx, provides a crucial metric for assessing the economic feasibility of different design options, making it essential for selecting the most cost-effective and technically viable configuration[30].

The food processing industry is characterized by its complexity and diversity. It spans a wide range of food products, processing techniques, preservation strategies, and distribution networks. This inherent complexity presents a variety of challenges: increasing consumer expectations, the need for product customization, and growing concerns about sustainability and resource efficiency.

In response to these evolving demands, the industry is undergoing a transformation, re-evaluating its practices in order to improve productivity, ensure consistent quality, reduce environmental impact, and better meet market needs. In recent years, this transformation has been significantly shaped by the integration of advanced technologies and digital solutions.

One of the most promising developments in this context is the Digital Twin (DT), a concept strongly associated with the broader movement of Industry 4.0 [1]. A digital twin can be described as a dynamic, virtual representation of a physical system, continuously updated through real-time data from its operating environment. Unlike static models, a DT evolves alongside the real system, enabling the monitoring of current states, the prediction of future behaviors, and the support of decision-making processes across multiple time scales.

More specifically, digital twins combine mathematical modeling, simulation tools, and real-time data integration to provide a deeper understanding of the system’s behavior. This includes estimating hard-to-measure variables, improving process visibility, and identifying optimization opportunities. In the food industry, where real-time insights, quality control, and efficiency are critical, such capabilities are particularly valuable.

The growing interest in digital twin technology is fueled by its versatile applications. It can support process optimization, by identifying optimal operating conditions or design parameters; real-time monitoring, through the integration of historical, live, and predictive data; and advanced control, by linking virtual and physical systems to maintain stability and product quality, even in the presence of process disturbances [1].

Although the concept of digital twins is relatively recent, it is rapidly gaining traction across various industrial sectors, including food manufacturing, due to its potential to merge engineering knowledge, data analytics, and usability in a single intelligent framework [28].

This thesis contributes to this field by exploring the application of digital twin technology in smarter food manufacturing, with a specific focus on the multi-effect evaporation process for tomato concentrate production. By developing and validating a digital twin model in AVEVA Dynamic Simulation software, this work investigates not only steady-state and economic performance, but also the dynamic behavior of the process during start-up and shutdown operations. The results aim to demonstrate how such models can support process understanding, control, and optimization in a modern, data-driven industrial environment.

Optimization of multiple-effect evaporation systems in tomato processing has attracted considerable attention in recent engineering studies. Simpson et al. (2008) [27] pioneered an approach that integrates quality and economic metrics by optimizing the number of effects using both Net Present Value (NPV) and lycopene retention as a product quality indicator. Their Excel-based model suggests that, while total cost minimization favors a four-effect configuration, the inclusion of lycopene retention in the NPV evaluation shifts the optimum to three effects.

Another example of optimization of a multiple-effect evaporator is provided by Ganjeizadeh et al. (2020) [13]. The article presents a MATLAB-based mathematical model to evaluate energy performance, specifically steam economy, across configurations of three, five, and seven effects. This study highlights the energy advantages of increased effects but does not consider quality parameters.

In parallel, several studies have explored the effect of processing conditions on the quality of tomato products. The chemical stability of bioactive compounds, such as lycopene, vitamin C, and pectin, is known to be strongly influenced by thermal treatment. For example, Al-Kafrawy et al. (2022) [2] investigated the impact of hot-break processing and triple-concentration on tomato paste, highlighting changes in physicochemical properties and nutrient retention. Similarly, Xu et al. (2018) [40] examined how different processing methods, including hot-break and cold-break techniques, affect color, viscosity, and bioactive compound retention in tomato products. These contributions underline the necessity of balancing economic and energy considerations with product quality preservation.

More recently, the integration of digital technologies into evaporation systems has opened new avenues for process optimization and monitoring. In particular, Soares et al. (2019) [28] developed a digital twin for industrial multi-effect evaporation of sugarcane juice, demonstrating its potential to enhance process control,

predictive maintenance, and operational safety. While this study focused on sugarcane processing, it illustrates the value of digital twins for simulating complex evaporation systems.

Building on these advances, the present work extends the application of digital twin technology to tomato paste production. It combines techno-economic optimization with dynamic simulation to identify the configuration that minimizes total costs while preserving product quality. Specifically, the dynamic simulation is realized with the software AVEVA Dynamic Simulation to reproduce realistic start-up and shutdown operations. This integration of cost analysis, quality assessment, and dynamic digital simulation provides a tool for enhanced process understanding, safer operations, and more sustainable tomato paste production.

2. Materials and Methods

This section describes the methodology employed for the design and optimization of a multiple-effect evaporation process aimed at concentrating tomato juice into tomato paste. The objective of this work is the development of a Digital Twin, a mathematical model designed to reproduce the dynamic behavior of a real industrial process. This model is implemented using AVEVA Dynamic Simulation (Dynamicsim), a specialized dynamic simulation software that enables the accurate representation and analysis of time-dependent process responses under various operating conditions. This modeling approach not only supports design and operational optimization, but also enables the estimation of key process variables that are otherwise difficult or impossible to measure directly, thereby providing deeper insight into the system’s actual performance [28].

The analysis starts by defining the composition of the tomato juice used as the feed stream in the simulation, as this directly influences the thermodynamic and physical properties relevant to the process. Subsequently, the multistage evaporation system is described in detail, including the configuration of each stage and the governing principles. This involves formulating and applying mass and energy balance equations for each effect. The primary objective of this phase is to identify the optimal number of evaporation stages by conducting an economic analysis, enabling a cost-benefit comparison among different design configurations. Once the optimal number of effects is determined through the economic assessment, the simulation can proceed in the Dynamicsim environment, where the process is modeled and dynamically analyzed by performing specific start-up and a shut-down procedures.

2.1. Feed Composition

The typical composition of tomato juice per 100 grams is reported in Table 1 [18]. The product is predominantly water with small amounts of carbohydrates, proteins and fibers. The high water content justifies the use of evaporation as concentration method. As mentioned in Section 1— *Introduction*, the bioactive compounds Lycopene, Pectin and Ascorbic Acid (Vitamin C) affect the color, nutritional and sensory quality, viscosity and sensitivity to thermal degradation of the juice. It is therefore essential to tightly monitor the operating conditions to avoid compromising the integrity of the final product [40].

Table 1: Composition of tomato juice per 100 g

Water	Protein	Fat	Carbohydrates	Pectin	Lycopene
94 g	0.9 g	0.1 g	3.3 g	0.8 g	5 mg
Phosphorus	Calcium	Iron	Potassium	Vitamin E	Vitamin A
19 mg	7 mg	0.7 mg	237 mg	0.54 mg	0.25 mg
Vitamin B1	Vitamin B2	Vitamin C	Vitamin B3	Total Folate	–
0.05 mg	0.02 mg	12.7 mg	0.6 mg	15 µg	–

The composition reported in Table 1 can be implemented in Dynamicsim as the feed mixture for the evaporation process. However, since not all components are available in the Dynamicsim component library, some of them — Fat, Pectin, Lycopene, Vitamin A [10], Vitamin B1 [38], Vitamin B2 [37], Vitamin B3 [36], and Folate [9] — are introduced as pseudocomponents in order to represent their physical and chemical behavior. To ensure the accuracy of the simulation, to each pseudocomponent key physical properties are assigned, including molecular weight, standard liquid density, and normal boiling point (Table 2). This approximation allows a realistic representation of the tomato concentrate process, while maintaining consistency in mass and energy balances.

Table 2: Physical properties of selected pseudocomponents implemented in Dynsim

Component	Molecular Weight (kg/kmol)	Std Liquid Density (kg/m ³)	NBP (K)
Fat	885.43	907.8	827.15
Pectin	194.14	1508	688.65
Lycopene	536.89	889	934.05
Vitamin A	286.46	993	396.15
Vitamin B1	265.35	1377	523.15
Vitamin B2	376.36	1211	553.15
Vitamin B3	123.11	1473	510.00
Total Folate	15	1470.4	523.15

2.2. Data and Problem Setting

This study addresses a design problem related to a feed-forward multiple-effect evaporation system for the concentration of tomato juice. The goal is to determine the optimal number of evaporation effects N_{effects} required to concentrate a given feed stream of tomato juice from an initial solids concentration of 5 °Brix to a final concentration of approximately 30 °Brix.

2.2.1 Multistage Evaporation Process

To identify the most suitable configuration, the evaporator system is designed and evaluated for a range of one to five effects, in accordance with the design range discussed in 1— *Introduction*. This stepwise approach enabled the comparison of different setups from both an operational and economic standpoint. The objective is to perform an economic optimization by minimizing the total cost, which includes both capital expenditures and operating expenses. A schematic representation of the process is provided in Figure 4, offering a visual overview of the system layout.

The diagram highlights the main process streams, including:

- **Light blue arrows:** represent the flow of vapor ($V_0, V_1, V_2, V_3, V_4, V_5$);
- **Red arrows:** indicate the tomato stream ($L_0, L_1, L_2, L_3, L_4, L_5$);
- **Black arrows:** show the condensate from each effect.

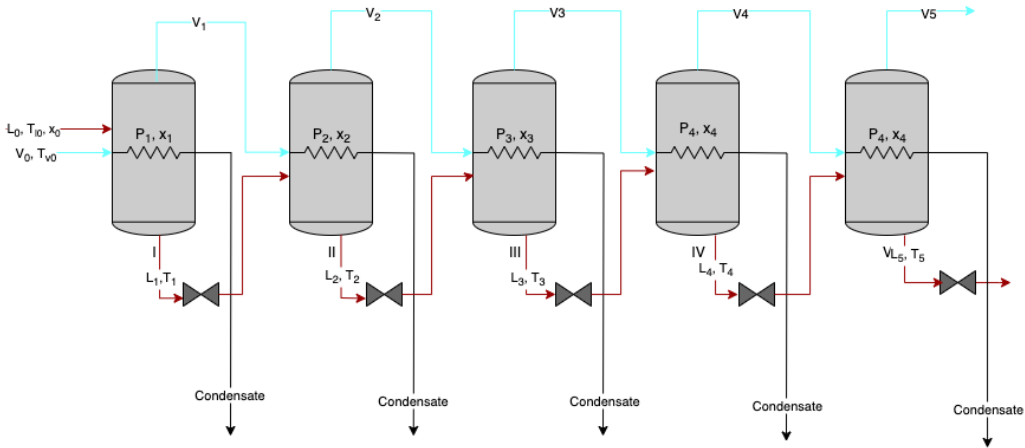


Figure 4: Multi-stage Evaporation Process

The input data used for the analysis are presented and explained step by step in the following tables, which summarize the assumptions, process specifications, and physical parameters applied throughout the design procedure.

A 50000 kg/h stream L_0 of tomato juice with a dissolved solid concentration x_0 of 5 % w/w has to be concentrated in a co-current N_{effects} evaporator [27]. The feed inlet temperature T_{i0} is 90 °C. This elevated temperature is a result of the pretreatment steps to which the tomato juice is subjected prior to evaporation. After grading, washing and sorting, tomatoes undergo a mechanical chopping process known as "breaking," which can be

performed using either a cold-break or hot-break technique. In hot-break processing, the tomato pulp is rapidly heated to approximately 82–93°C before extraction. This method helps preserve pectins in the product, resulting in a higher viscosity, improved consistency, and enhanced stability of the final concentrate [23]. The other inlet stream is the steam, used as the heating medium for the first effect, which has a saturation temperature T_{v0} of 129 °C and a pressure P_{v0} of 260 kPa [27].

Tables 3, 4 and 5 summarize the key input parameters and physical properties employed in the modeling and simulation of the multistage evaporation system. Table 3 reports the main input data, including the mass flow rate, temperature, and solid concentration of the tomato feed, along with the temperature of the inlet steam [27]. Table 4 presents the physical properties used in the analysis, such as the specific heat capacity of the tomato solution [25], assumed constant throughout the process, and the evaporation enthalpy of the inlet steam ($T = 129$ °C, $P = 260$ kPa) by interpolation from standard steam tables [20]. Finally, Table 5 details the design parameters and physical properties for each evaporator effect (from the first to the fifth), specifying the heat exchange area, overall heat transfer coefficient, and the enthalpy change associated with each evaporation stage [27]. These data collectively serve as the foundation for the thermodynamic and economic evaluation of the system.

Table 3: Input Data

Process Variable	Value	Unit
L_0	50000	kg/h
T_{l0}	90	°C
x_0	0.05	kg/kg
T_{v0}	129	°C
P_{v0}	260	kPa

Table 4: Physical Properties

Property	Value	Unit
c_{pl}	1.17	kcal/kg/K
$\Delta H_{ev}^{\text{steam}}$	651.39	kcal/kg

Table 5: Physical Properties and Design Data for Evaporator Effects

Effect	Property	Value	Unit
First	A_1	209	m ²
	$\Delta H_{ev,1}^{\text{vap}}$	636.19	kcal/kg
	U_1	1074.21	kcal/m ² /h/K
Second	A_2	209	m ²
	$\Delta H_{ev,2}^{\text{vap}}$	628.19	kcal/kg
	U_2	1617.4	kcal/m ² /h/K
Third	A_3	209	m ²
	$\Delta H_{ev,3}^{\text{vap}}$	621.69	kcal/kg
	U_3	2025.67	kcal/m ² /h/K
Fourth	A_4	209	m ²
	$\Delta H_{ev,4}^{\text{vap}}$	615.19	kcal/kg
	U_4	2433.94	kcal/m ² /h/K
Fifth	A_5	209	m ²
	$\Delta H_{ev,5}^{\text{vap}}$	608.69	kcal/kg
	U_5	2842.21	kcal/m ² /h/K

To carry out the design and optimization of the multiple-effect evaporation system, the following assumptions were made to simplify the analysis and ensure procedural consistency [22],[25]:

- All evaporation effects are assumed to have the same heat exchange surface area.
- The steam flow rate is selected as a manipulated variable to facilitate convergence during the iterative design process.
- The design calculations are performed iteratively, solving one effect at a time in a sequential manner.
- The tomato juice/paste in the evaporator is assumed to be completely mixed.
- The specific heat c_p of tomatoes juice at 5% concentration is taken as 1.17 kcal/kg/K and is assumed constant during the process.
- No heat is lost by radiation or convection.

Once all the relevant input data and design specifications have been defined, the calculation procedure is carried out according to the following procedure, which involves a sequential evaluation of thermal and mass parameters for each evaporator effect, starting from the first stage [22]. The steps are as follows:

1. Heat transfer and Temperature Difference:

Given the specified duty for the first effect, the temperature difference across the effect is calculated based on the global heat transfer equation:

$$V_0 \cdot \Delta H_{ev}^{steam} = U_1 \cdot A_1 \cdot \Delta T_1 \quad (1)$$

This step establishes the driving force for the heat exchange and is crucial for determining the boiling temperature in the first effect.

$$\Delta T_1 = \frac{V_0 \cdot \Delta H_{ev}^{steam}}{U_1 \cdot A_1} \quad (2)$$

2. Boiling Temperature of the solution:

Once the temperature drop is known, the boiling temperature of the product in the first effect can be estimated as:

$$T_1 = T_{v_0} - \Delta T_1 \quad (3)$$

3. Mass and Energy Balances:

The mass and energy balances allow the determination of flow rates and temperature profiles in each effect:

$$\begin{cases} L_0 = L_1 + V_1 & (4a) \\ L_0 \cdot c_{pl} \cdot T_{l_0} + V_0 \cdot \Delta H_{ev}^{steam} = L_1 \cdot c_{pl} \cdot T_1 + V_1 \cdot (c_{pl} \cdot T_1 + \Delta H_{ev,1}^{vap}) & (4b) \end{cases}$$

$$\begin{cases} V_1 = L_0 - L_1 & (5a) \\ L_0 \cdot c_{pl} \cdot T_{l_0} + V_0 \cdot \Delta H_{ev}^{steam} = L_1 \cdot c_{pl} \cdot T_1 + (L_0 - L_1) \cdot (c_{pl} \cdot T_1 + \Delta H_{ev,1}^{vap}) & (5b) \end{cases}$$

$$\begin{cases} V_1 = L_0 - L_1 & (6a) \\ L_1 = \frac{L_0 \cdot c_{pl} \cdot T_{l_0} + V_0 \cdot \Delta H_{ev}^{steam} - L_0 \cdot (c_{pl} \cdot T_1 + \Delta H_{ev,1}^{vap})}{-\Delta H_{ev,1}^{vap}} & (6b) \end{cases}$$

4. Solute Concentration:

A mass balance on the solute allows the calculation of the outlet concentration, a critical parameter for monitoring the concentration progression throughout the system:

$$L_0 \cdot x_0 = L_1 \cdot x_1 \quad (7)$$

$$x_1 = \frac{L_0 \cdot x_0}{L_1} \quad (8)$$

5. Boiling Point Elevation (BPE):

The presence of solutes causes an elevation in the boiling point, which must be considered when calculating the true operating temperature [27]:

$$\Delta T_{eb,1} = 0.175 \cdot x_1^{1.11} \cdot e^{3.86x_1} \cdot P_1^{0.43} \quad (9)$$

6. Vapor Pressure Calculation:

The pressure corresponding to the boiling temperature is estimated using an extended Antoine-type correlation. The coefficients used in this correlation are reported in Table 6.

$$\ln(P_{\text{ev}} [\text{Pa}]) = \frac{C_1}{T [\text{K}]} + C_2 + C_3 \cdot T + C_4 \cdot T^2 + C_5 \cdot T^3 + C_6 \cdot \ln(T) \quad (10)$$

Table 6: Vapor pressure correlation coefficients

C_1	C_2	C_3	C_4	C_5	C_6
-5.8002206×10^3	1.3914993	$-4.8640239 \times 10^{-2}$	4.1764768×10^{-5}	$-1.4452093 \times 10^{-8}$	6.5459673

7. Extension to subsequent effects:

The same approach is then applied recursively to each subsequent evaporator stage. As intermediate variables (V_i , T_i , L_i , x_i) depend on the results from the previous effect, an iterative method is required to ensure consistency throughout the train of effects.

To ensure the global mass balance is satisfied, the following objective function is used:

$$F_{\text{obj}} = V_{\text{tot,spec}} - V_{\text{tot,calc}} \quad (11)$$

Where [27]:

$$V_{\text{tot,spec}} = 40955.76 \text{ kg/h} \quad (12)$$

And

$$V_{\text{tot,calc}} = \sum_{i=1}^5 V_i \quad (13)$$

The iterative loop adjusts variables (typically L_1 or T_1) until F_{obj} reaches a defined convergence threshold ($V_{\text{tot,spec}} = V_{\text{tot,calc}}$). This ensures that the evaporation system meets the required performance target under the imposed design conditions.

2.3. Costs Analysis

Cost estimation is a crucial component of process design, providing the basis for assessing both the technical feasibility and economic viability of a proposed system. The estimation of capital and operating expenses allows for informed decision-making and optimization during the early stages of project development. In this section, the methodology applied to estimate the costs associated with the multiple-effect evaporator system is presented. This includes determining equipment costs through empirical correlations, which relate key design parameters to investment requirements. To reflect current economic conditions, cost adjustments are performed using the Chemical Engineering Plant Cost Index (CEPCI), accounting for inflation and market fluctuations. Additionally, operational costs are estimated based on steam consumption, as it represents a significant portion of ongoing expenses in evaporation processes. This analysis does not explore cost modeling in depth, since engineering and construction costs, working capital, contingencies and maintenance costs of the plant are neglected. However, this study offers a sufficiently accurate estimation framework for the specific purpose of identifying the optimal number of evaporator effects.

2.3.1 Capital Expenditure (CapEx)

Capital expenditures, as mentioned in Section 1— *Introduction*, represent the initial investment required for the purchase and installation of process equipment. In the context of this study, CapEx estimation focuses on calculating equipment costs based on size and operating conditions, using empirical cost correlations commonly adopted in chemical engineering design.

The base purchased cost for process equipment is estimated using the following empirical correlation:

$$C_p^0 = \exp(K_1 + K_2 \cdot \log A + K_3 \cdot (\log A)^2) \quad (14)$$

where:

- C_p^0 : purchased equipment cost in 2001 USD (carbon steel, atmospheric pressure),
- A : size or capacity parameter of the equipment (e.g., heat transfer area in m^2),

- K_1, K_2, K_3 : empirical constants specific to the equipment type (Table 7).

For the specific case of a **long-tube evaporator**, the following values are used, as reported in Table A.1 of Appendix A in *Analysis, Synthesis, and Design of Chemical Processes* [34]:

Table 7: Empirical constants for long-tube evaporators

K_1	K_2	K_3
4.642	0.3698	0.0025

The bare module factor F_{BM} is determined from Figure A.19, using the equipment classification provided in Table A.6 reported in Table A.1 of Appendix A in *Analysis, Synthesis, and Design of Chemical Processes* [34]. The bare module cost for evaporators is estimated using the correlation provided in Table A.5 of Appendix A [34]:

$$C_{BM} = C_p^0 \cdot F_{BM} \cdot F_P \quad (15)$$

where:

- C_{BM} : bare module cost [USD],
- C_p^0 : base purchased cost in 2001 USD (carbon steel, atmospheric pressure),
- F_{BM} : bare module factor (installation, material, labor),
- F_P : pressure factor.

For the case of long-tube evaporators, the values in Table 8 are used:

Table 8: Bare module and pressure factor for long tubes evaporators

F_{BM}	F_P
3.0	1.25

To update the cost from the base year (2001) to current economic conditions, the CEPCI index is used [34]. This correction ensures that the cost estimates reflect current market conditions, compensating for the effects of inflation over time:

$$C_2 = C_1 \cdot \left(\frac{I_2}{I_1} \right) \quad (16)$$

where:

- C_2 : updated cost at present (target) year,
- C_1 : known cost at base year (here, $C_1 = C_{BM}$),
- I_1 : CEPCI index at base year (2001) = 397,
- I_2 : CEPCI index at year of interest (e.g., 2024) = 800.

The total capital expenditure is calculated by multiplying the updated bare module cost, C_2 , by the number of effects of the evaporator system N_{effects} :

$$\text{CapEx } [\$] = C_2 \cdot N_{\text{effects}} \quad (17)$$

2.3.2 Operating Expenditure (OpEx)

Operating expenditures, as mentioned in Section 1— *Introduction*, refer to the ongoing costs required to run the process under normal operating conditions. In the context of this study, OpEx estimation considers the cost of steam used for evaporation.

The operating expenditure is estimated based on the consumption of fresh steam, V_0 [kg/h], the annual operating hours, the total plant lifetime, and the unit cost of steam. The annual operating time is assumed to be approximately 1,680 hours, calculated as 70 days per year of continuous operation. This assumption reflects the seasonal nature of tomato processing, which is typically concentrated between mid-July and late September, when tomatoes naturally ripen. During this period, factories operate 24/7 to process the raw material within a limited time window [24].

The economic lifetime of the evaporation system is assumed to be 15 years, in line with standard industrial practice for multi-effect evaporators in the food processing sector. Although Simpson et al. [27] do not explicitly define a fixed equipment lifetime, their Net Present Value (NPV) model is based on a multi-year evaluation horizon, denoted as parameter m (project shelf life, in years). This modeling approach supports the assumption of a long-term operational horizon, typically ranging from 10 to 20 years in industrial applications. Therefore, adopting a 15-year lifetime for the economic analysis is both reasonable and consistent with their methodology. Regarding the steam cost, according to Table 8.3 in Chapter 8 of *Analysis, Synthesis, and Design of Chemical Processes* [34], it is estimated to be approximately 0.03 \$/kg, based on standard pricing data for industrial utilities. This estimate assumes the case of low-pressure steam without credit for power, meaning that no economic value is assigned to the electricity potentially generated during steam production.

$$\begin{aligned} \text{OpEx } [\$] &= V_0 \left[\frac{\text{kg}}{\text{h}} \right] \cdot 1,680 \left[\frac{\text{h}}{\text{y}} \right] \cdot 15 [\text{y}] \cdot 0.03 \left[\frac{\$}{\text{kg}} \right] \\ &= \underbrace{V_0 \cdot 1,680 \cdot 15}_{\text{total steam consumption [kg]}} \cdot 0.03 \left[\frac{\$}{\text{kg}} \right] \end{aligned} \quad (18)$$

To evaluate the economic performance of each evaporator configuration, the total costs are computed as the sum of capital expenditures and cumulative operating expenditures over the expected plant lifetime. Thus, the total costs over the project lifetime are calculated as:

$$\text{Total costs } [\$] = \text{CapEx} + \text{OpEx} \quad (19)$$

This approach allows for a straightforward comparison between different evaporator configurations by integrating both investment and operational perspectives into a single economic indicator.

2.4. Packaging heat exchanger

In addition to the evaporators system, a heat exchanger is included to raise the temperature of the final product stream from 50°C to 90°C. This temperature is required for packaging operations, as canned tomato paste is typically hot-filled at a minimum temperature of 90°C into cans. The product is then sealed without further heat treatment, passed through a water spray to remove any residue from the exterior, cooled, and finally packed [23]. To perform this heating step, the process vapor stream V_0 exiting the first evaporator, can be employed as the heating medium. This step is considered only to illustrate a possible energy recovery for the downstream filling operation and is not implemented in AVEVA Dynamic Simulation.

The design of the heat exchanger is carried out according to the following procedure:

1. Estimation of the thermal energy required to heat the tomato product stream

The thermal energy required to heat the concentrated tomato stream from 50°C (exit temperature of the N_{eff} -th evaporator) to 90°C (packaging temperature) was calculated as follows:

$$Q_{\text{needed}} = L_n \cdot c_{p,l} \cdot (T_{\text{pack}} - T_n) \quad (20)$$

where L_n and T_n represent, respectively, the flow rate and temperature of the liquid concentrated tomato stream exiting the N_{eff} -th evaporator.

2. Assessment of the thermal energy available from the vapor stream V_0

Assuming a final outlet temperature for the vapor stream T_v^{out} , the available energy was estimated as:

$$Q_{\text{available}} = V_0 \cdot c_{p,w} \cdot (T_{v0} - T_v^{\text{out}}) \quad (21)$$

3. Definition of the objective function

The objective function was defined to match the thermal energy required to heat the tomato product stream with the thermal energy available from the vapor stream V_0 :

$$F_{\text{obj}} = Q_{\text{needed}} - Q_{\text{available}} \quad (22)$$

4. Calculation of the required heat exchange area

Based on the final heat duty, temperature profiles, and an assumed global heat transfer coefficient U , the required heat exchange surface was calculated using:

$$A_{\text{HE}} = \frac{Q}{U \cdot \Delta T_{\text{lm}}} \quad (23)$$

where ΔT_{lm} is the log mean temperature difference (LMTD) between the hot and cold streams, calculated as:

$$\Delta T_{lm} = \frac{\Delta T_1 - \Delta T_2}{\ln\left(\frac{\Delta T_1}{\Delta T_2}\right)} \quad (24)$$

2.4.1 Packaging Heat Exchanger Cost Estimation

For this case, a **double-pipe heat exchanger** is selected and its cost is estimated using the same correlation applied for the evaporators, with empirical constants (Table 9) specific to this equipment type taken from Table A.1 of Appendix A in *Analysis, Synthesis, and Design of Chemical Processes* [34]:

Table 9: Empirical constants for double-pipe heat exchanger

K_1	K_2	K_3
3.3444	0.2745	-0.0472

The bare module cost is then estimated using equation A.4 of Appendix A [34]:

$$C_{BM} = C_p^0 \cdot F_{BM} \quad \text{with} \quad F_{BM} = B_1 + B_2 \cdot F_M \cdot F_P \quad (25)$$

where The constants B_1 and B_2 (Table 10) were taken from Table A.4 for double-pipe exchangers of Appendix A [34]:

Table 10: Bare factor's constants for double-pipe exchangers

B_1	B_2
1.74	1.55

The material factor F_M was obtained from Figure A.18 using the classification in Table A.3 of Appendix A [34]. For carbon steel construction, the value is:

$$F_M = 1.00$$

The pressure factor F_P is determined using Equation A.3:

$$\log_{10}(F_P) = C_1 + C_2 \cdot \log_{10}(P) + C_3 \cdot (\log_{10}(P))^2 \quad (26)$$

For double-pipe exchangers, all pressure constants are zero, accordingly from Table A.2 of Appendix A [34], so:

$$F_P = 1.00$$

Substituting into Equation (19):

$$F_{BM} = 1.74 + 1.55 \cdot 1.00 \cdot 1.00 = 3.29$$

And thus:

$$C_{BM} = C_p^0 \cdot 3.29$$

Finally, the cost is updated to current economic conditions using the CEPCI index:

$$C_{\text{updated}} = C_{BM} \cdot \left(\frac{I_2}{I_1}\right) = C_{BM} \cdot \left(\frac{800}{397}\right) \quad (27)$$

2.5. The Digital Twin

The digital reproduction, commonly referred to as a Digital Twin, enables the virtual modeling and analysis of the system's behavior under various design and operating conditions. The digital twin has been implemented only after the completion of the economic optimization phase, which identified the **three-effect configuration** as the most cost-effective setup (as it will be discussed in Subsection 3.2 — *Optimal Number of Effects* of Section 3 — *Results*). Therefore, all simulations are carried out on a three-effect evaporator, and the model is

designed to accurately reproduce the physical and thermodynamic behavior of the real system under this specific configuration. The main objective of this implementation is to create a virtual replica capable of supporting process control strategies and enabling the estimation of key process variables that are difficult to measure directly, providing valuable insights into both steady-state and dynamic responses.

Figure 5 illustrates the process flow diagram of the evaporation system as implemented in AVEVA Dynamic simulation (Dynsim). The simulation environment replicates the plant layout using various elements, including sources and sinks, evaporator effects (each consisting of a heat exchanger and a drum), control loops, and regulating valves.

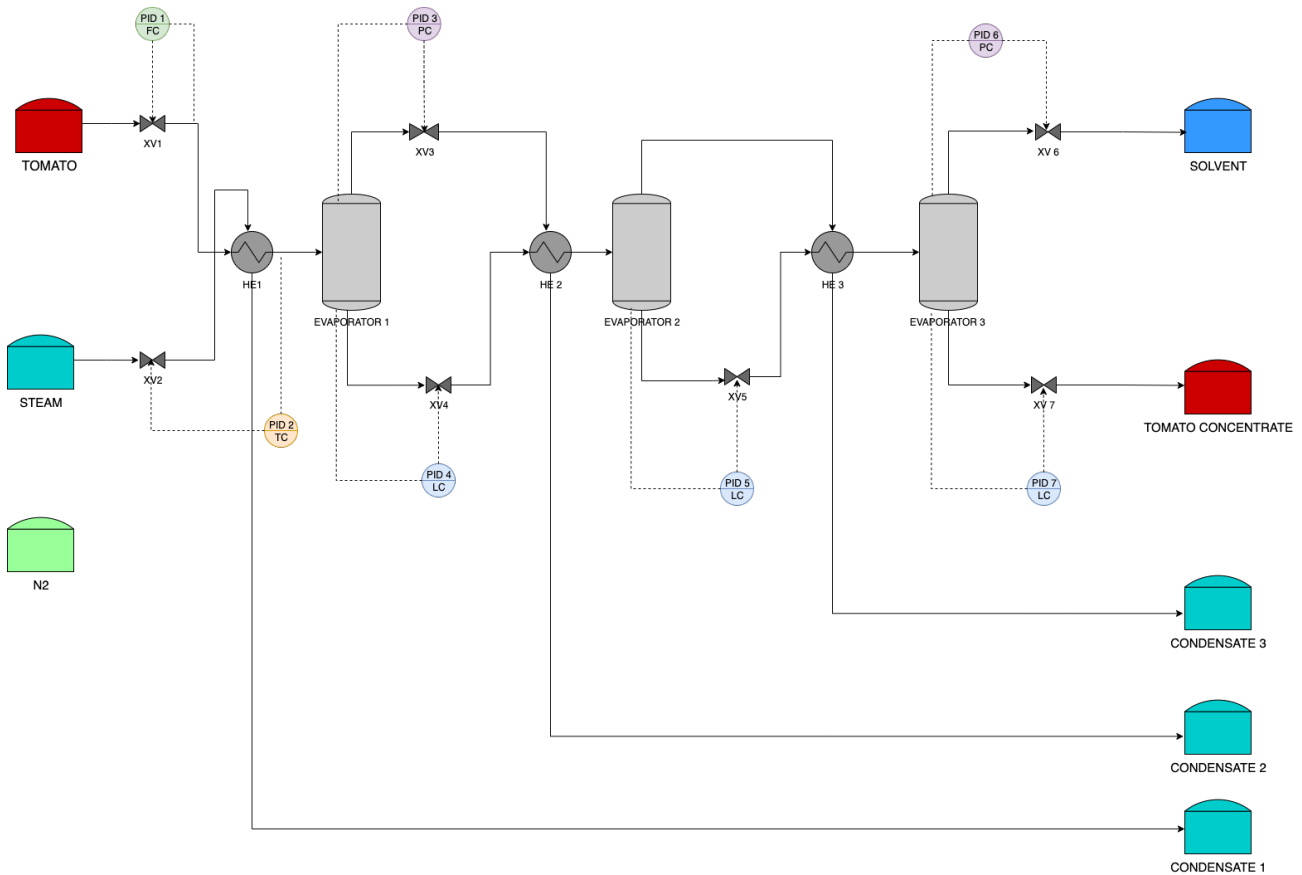


Figure 5: Process flow diagram of the three-effect evaporator system as implemented in Dynsim

2.5.1 Sources and Sinks

Within the DynSim environment, the model is structured using source and sink elements, which define the material and energy boundaries of the system. The source element introduces material or energy into the process, typically representing feed streams or utility inputs. Conversely, the sink element is used to remove material or energy from the system, modeling product or waste streams, and heat losses.

The source components are:

1. **Tomato Tank** (color: red): serves as the feed tank for tomato juice, providing the tomato juice that enters the process.
2. **Steam Tank** (color: light blue): represents the source of steam generation. The specific type and design of this component were not the focus in this context. In practice, the system could be connected to a boiler or a steam generator; however, it is considered here only as a generic steam supply.
3. **Nitrogen Virtual Tank** (color: green): consists of a virtual element used for initializing the system. It does not correspond to a physical tank but is necessary to define the initial conditions for the simulation start-up.

The sink elements are:

1. **Tomato Concentrate Tank** (color: red): represents the outlet of the concentrated tomato juice. In practice, a dedicated storage tank for tomato paste is not necessarily present at this stage, as the concen-

trate is often transferred directly to the sterilization and packaging line.

2. **Solvent Tank**(color: blue): collects the vapor phase (solvent) exiting the head of the third evaporator in the multi-effect evaporator system.
3. **Condensate Tanks** (color: light blue): collect the condensate streams from the three evaporator effects.

2.5.2 Evaporator effects

Each evaporator effect is modeled as a combination of:

1. **Heat Exchanger** (HE1, HE2, HE3): transfers the latent heat from condensing steam to the process feed
2. **Flash Drum** (EVAPORATOR 1, EVAPORATOR 2, EVAPORATOR 3): separates liquid concentrate from vapor produced by evaporation.

The dimensioning of the flash drum vessels within DynSim can be carried out by applying a residence time-based approach. A holdup time of approximately 5 minutes [32] is chosen to ensure that the product remains in the vessel long enough to effectively exchange heat with the heating medium and avoid thermal degradation of the critical bioactive compounds. To estimate the size of the vessels, the mass flow rate of the tomato stream is converted into a volumetric flow rate, assuming a density approximately equal to that of water. This simplification enables a straightforward calculation of the volume required to ensure the desired residence time. Each vessel is assumed to have a cylindrical shape with a fixed diameter, and based on the calculated volume, the corresponding height is determined. For safety and operational flexibility, a margin is added to the calculated height by increasing it by a few meters, in order to account for potential variations in flow conditions and to prevent overflowing during transient phases.

2.5.3 Valves and Control loops

A set of valves and control loops is implemented to regulate key process variables and ensure operational stability across the different effects.

Implemented valves:

- **Feed Valve** (XV1): regulates the inlet flow rate of tomato juice into the first evaporator effect.
- **Steam Valve**(XV2): controls the supply of steam entering the first effect to provide the necessary thermal energy.
- **Liquid Valves**(XV4, XV6, XV7): installed at the bottom of each flash drum to control the flow of concentrated liquid from one effect to the next.
- **Vapor Valves**(XV3, XV5): located at the top of the first and third drums allowing the vapor produced in each effect to flow toward the subsequent heat exchanger.

Implemented Proportional Integral Derivative (PID) controllers:

- **Tomato Feed Flow Controller**(PID1): reverse flow controller that maintains the desired feed rate of tomato juice entering the system.
- **Steam Controller**(PID2): reverse temperature controller that adjust the flow of steam to sustain proper heat supply in the first effect.
- **Level Controllers** (PID4, PID6, PID7): direct level controllers used in each effect to maintain the liquid level inside each drum within specified operating ranges.
- **Pressure Controllers** (PID3, PID5): direct pressure controllers that in each effect, except for the second, regulate the internal pressure and ensure that the proper boiling temperature is maintained. The second effect operates at the pressure resulting from the upstream and the downstream and is not actively controlled.

2.6. Dynamic Scenarios: Start-Up and Shutdown Procedures

To assess the system’s behavior during key transitional phases, two specific dynamic scenarios were implemented within the DynSim environment: a controlled *start-up* and a safe *shut-down* procedure. These scenarios were scripted using sequential control logic and executed through DynSim’s command scripting interface, simulating real-world operating strategies.

2.6.1 Start-up Scenario

The start-up scenario is designed to gradually bring the evaporator system to full operating conditions, ensuring thermal stability and reducing mechanical and thermal stress.

During the first two minutes, all process valves are closed, except for the steam valve (XV2). This choice is aimed to prevent the premature introduction of the liquid, which could cause thermal shock or unstable boiling, and ensure an initial warming of the first effect before the introduction of the tomato feed. The steam controller (PID2) operates in manual mode with an initial setpoint of 100 °C, with a partial opening of the valve (XV2) of 50%.

After the pre-heating, the feed controller (PID1) switches to automatic mode, allowing a regulated and gradual admission of tomato juice into the first effect. Simultaneously, the steam valve opening is gradually increased from 50% to 75% over five minutes to enable a smooth and controlled temperature increase.

Once the internal temperature of the first effect exceeds 98 °C, the setpoint of PID2 is updated to its target steady-state value of 96.243 °C; PID2 returns to automatic mode, gradually stabilizing until the system reaches steady-state conditions. Figure 6 illustrates a summary of the start-up procedure.

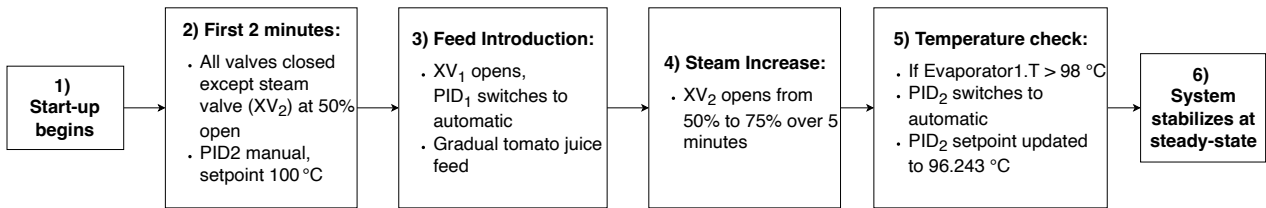


Figure 6: Start-up Scenario summary

2.6.2 Shut-down Scenario

The shut-down scenario is designed to drain the evaporator system, ensuring the safe emptying of the drums.

The procedure begins with the loading of two predefined initial conditions: the previously established steady-state configuration and the transition of all relevant controllers (PID1, PID2, PID4, PID5, PID7) into manual mode. The related action is the fully closing of the feed and steam inlets valves (XV1 and XV2) and simultaneously opening of the bottom outlet valves of the evaporator drums (XV4, XV5, XV7) to initiate draining.

The shutdown process is completed once all levels fall below a predefined threshold of 0.05, indicating that the vessels are effectively emptied and the unit is ready for maintenance or restart. Figure 7 illustrates a summary of the shut-down procedure.

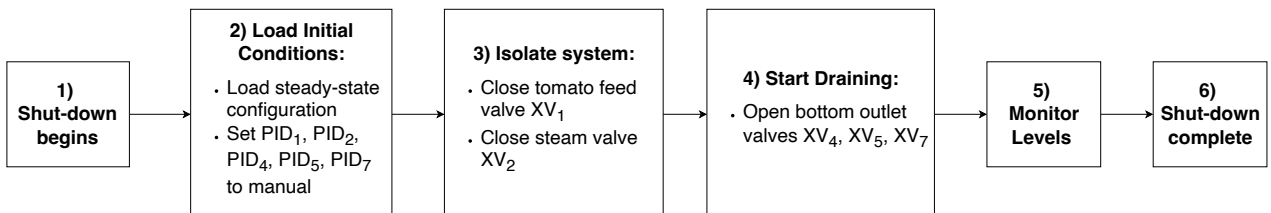


Figure 7: Shut-down Scenario summary

3. Results

This section presents and discusses the results obtained by applying the methodology outlined in Section 2—*Materials and Methods*. The analysis begins with the evaluation of the economic data, focusing on the cost estimation results that form the basis for determining the optimal number of effects in the multi-stage evaporation process. This decision is supported by a comparative assessment of total costs, balancing capital and operating expenditures to identify the most cost-effective configuration.

Next, a sensitivity analysis is performed to examine how variations in key input parameters influence the economic outcome and affect the reliability of the selected configuration. This step is essential to ensure the robustness of the result under realistic operating uncertainties.

Finally, the dynamic behavior of the system is analyzed through simulation, focusing on the evolution of temperature, pressure, and liquid levels within each evaporator under transient conditions. Particular attention is given to the start-up and shut-down phases, which are critical for assessing system stability and control performance, providing insight into the system’s responsiveness, control requirements, and potential operational challenges.

3.1. Costs Analysis Results

One of the fundamental design decisions in configuring a multi-effect evaporator system is the determination of the optimal number of effects, as it directly impacts both capital and operational costs. Increasing the number of effects in a multi-stage evaporator generally reduces steam consumption and, consequently, the operating costs. However, this improvement comes with a higher capital investment. To assess the economic trade-off between efficiency and investment, five system configurations, ranging from one to five effects, are analyzed. In Table 11, the results of the cost analysis are reported and graphically illustrated in Figure 8.

Table 11: Economic Evaluation for Different Numbers of Evaporator Effects

Number of Effects	CAPEX [mln USD]	V_0 [kg/h]	OPEX [mln USD]	Total Cost [mln USD]
1	2.46	33,985.71	25.69	28.16
2	4.93	17,156.46	12.97	17.90
3	7.39	11,534.34	8.72	16.11
4	9.86	8,746.77	6.61	16.47
5	12.32	7,091.72	5.36	17.69

The total costs reach their minimum at three effects, confirming that the **three-effect evaporator** achieves the lowest overall cost, making it the most economically advantageous solution.

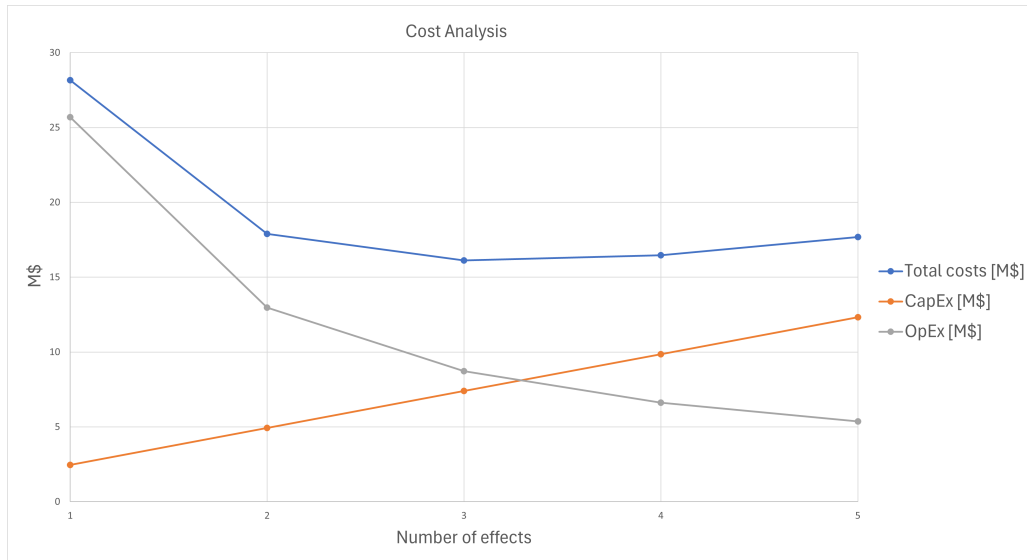


Figure 8: Comparison of capital, operational and total costs across evaporator configurations from one to five effects

3.2. Optimal Number of Effects

Having identified the three-effect configuration as the most economically advantageous solution through the cost analysis, this subsection provides a more detailed examination of its design and operational features. Figure 9 illustrates the optimal evaporation system configuration, consisting of three effects arranged in a feed-forward operating mode.

The diagram highlights the main process streams, including:

- **Light blue arrows:** represent the flow of vapor (V_0, V_1, V_2, V_3);
- **Red arrows:** indicate the tomato stream (L_0, L_1, L_2, L_3);
- **Black arrows:** show the condensate from each effect.

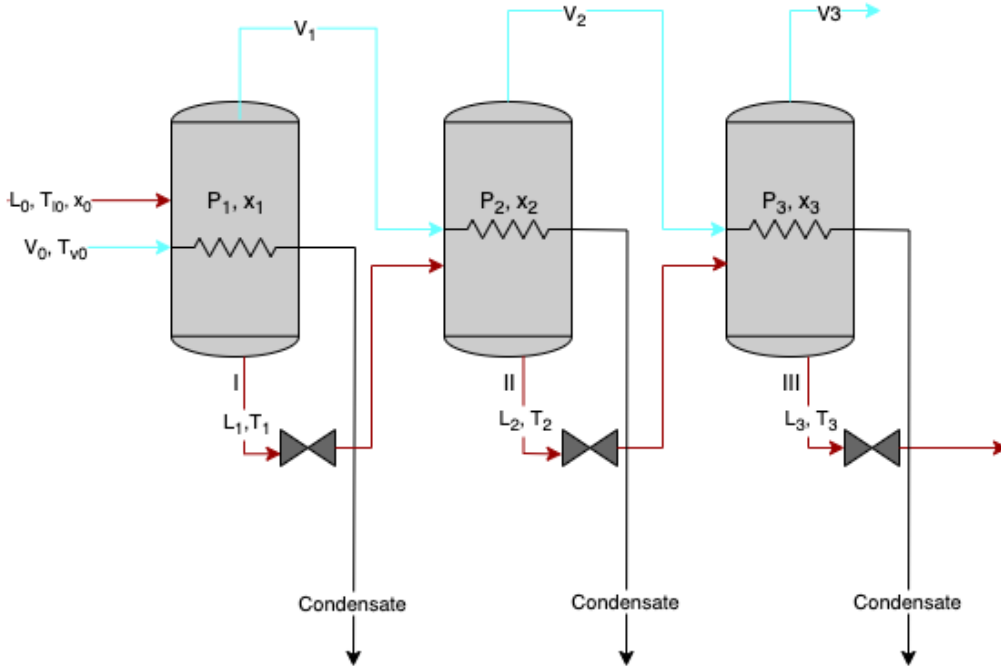


Figure 9: Three-effects Evaporation Process

Table 12 presents all key input, design, and calculated data for the three-effect evaporator configuration. The results of mass and energy balances, reported in Table 12 are the following:

- In the **first effect**, fresh steam ($V_0 = 11,534.34$ kg/h) heats the feed, resulting in $V_1 = 12,012.98$ kg/h of evaporated water and a liquid outflow of $L_1 = 37,987.02$ kg/h with a solids concentration of $x_1 = 6.58\%$.
- In the **second effect**, V_1 is used as heating steam. It produces $V_2 = 13,888.40$ kg/h of vapor and a liquid stream $L_2 = 24,098.62$ kg/h with $x_2 = 10.37\%$.
- The **third effect** further concentrates the product to $x_3 = 27.64\%$, with $V_3 = 15,054.38$ kg/h of vapor produced and a final liquid stream $L_3 = 9,044.24$ kg/h.

As expected, the boiling point elevation increases throughout the evaporation process due to the progressive rise in solute concentration. The system operates under vacuum conditions for the entire duration of the process, with the pressure gradually decreasing from the first to the third effect. This pressure gradient is accompanied by a corresponding decrease in temperature across the effects, which contributes to preserving the quality of the final product.

Table 12: Summary of Input and Calculated Parameters for the Three-Effect Evaporator: Values in **bold** indicate system inputs, distinguishing them from calculated outputs.

Parameter	Value	Unit	Note
General and Physical Data			
Feed flow rate (L_0)	50,000	kg/h	input
Total vapor produced (V_{tot})	40,955.76	kg/h	sum of V_1, V_2, V_3
Initial concentration (x_0)	0.05	kg/kg	feed solids
Liquid temperature (T_{L0})	90	°C	inlet
Steam temperature (T_{v0})	129.1	°C	heating steam
Liquid heat capacity (c_p)	1.17	kcal/kg/K	assumed constant
Steam latent heat ($\Delta H_{\text{ev,steam}}$)	651.39	kcal/kg	
Design Parameters			
Heat transfer area per effect (A)	209	m ²	constant
$\Delta H_{\text{ev},1} / \Delta H_{\text{ev},2} / \Delta H_{\text{ev},3}$	636.96 / 628.19 / 621.69	kcal/kg	per effect
$U_1 / U_2 / U_3$	1074.21 / 1617.4 / 2025.67	kcal/m ² /h/K	heat transfer coefficients
Effect-by-Effect Operational Results			
Effect	1st	2nd	3rd
Temperature drop ΔT [°C]	33.47	22.64	20.61
Boiling point elevation ΔT_{eb} [°C]	1.50	1.90	6.95
Boiling temperature T_v [°C]	94.13	69.60	42.04
Liquid outlet flow L [kg/h]	37,987.02	24,098.62	9,044.24
Vapor flow V [kg/h]	12,012.98	13,888.40	15,054.38
Solids concentration x [kg/kg]	0.0658	0.1037	0.2764
Temperature T [°C]	95.63	71.49	48.99
Temperature T [K]	368.78	344.64	322.14
Pressure [atm]	0.855	0.328	0.116
Pressure [Pa]	86,603	33,274	11,743

The amount of fresh steam introduced into the system, obtained from the iterative procedure, denoted as V_0 , corresponds to:

$$V_0 = 11,534.34 \text{ kg/h}$$

This steam supplies the thermal energy required by the first effect. The vapor generated in the first effect is then reused as the heating medium for the second effect, and this cascading utilization continues throughout the system. The total vapor produced by evaporation across all the three effects is:

$$V_{\text{tot}} = V_1 + V_2 + V_3 = 40,955.76 \text{ kg/h}$$

From this, the steam economy of the system is calculated as:

$$\text{Steam Economy} = \frac{V_{\text{tot}}}{V_0} = \frac{40,955.76}{11,534.34} \approx \mathbf{3.55}$$

Steam economy is a key performance indicator in evaporator design, defined by the ratio of evaporated solvent to steam consumption, and is strongly influenced by the number of effects, the boiling point elevation, and the effectiveness of heat recovery across the stages [15]. In this case, a steam economy of approximately 3.55 signifies that for every kilogram of fresh steam supplied, about 3.55 kilograms of water are evaporated, demonstrating a substantial degree of energy reuse and confirming the efficiency of the selected three-effect configuration.

3.3. Sensitivity Analysis on the Optimal Number of Effects

To evaluate the robustness of the optimal three-effect configuration, a sensitivity analysis is performed by varying key input parameters and examining their impact on the economically optimal number of effects. This approach helps to verify whether the identified optimal design remains valid under different operating conditions and uncertainties.

3.3.1 Variation in Feed Flow Rate

The first part of the analysis investigates the effect of changes in the feed flow rate. Five scenarios are considered, corresponding to variations of -60% , -40% , -20% , $+20\%$, and $+40\%$ relative to the nominal feed flow rate L_0 . For each scenario, the total cost is recalculated for evaporator configurations ranging from one to five effects. The results, illustrated in Figure 10, show that the optimal number of effects remains three in most cases. However, when the feed flow is reduced by 60%, a two-effect configuration becomes more economically convenient, and when it is increased by 40%, a four-effect configuration is favored. These results indicate that the optimal design is generally robust but sensitive to substantial changes in the feed flow rate.

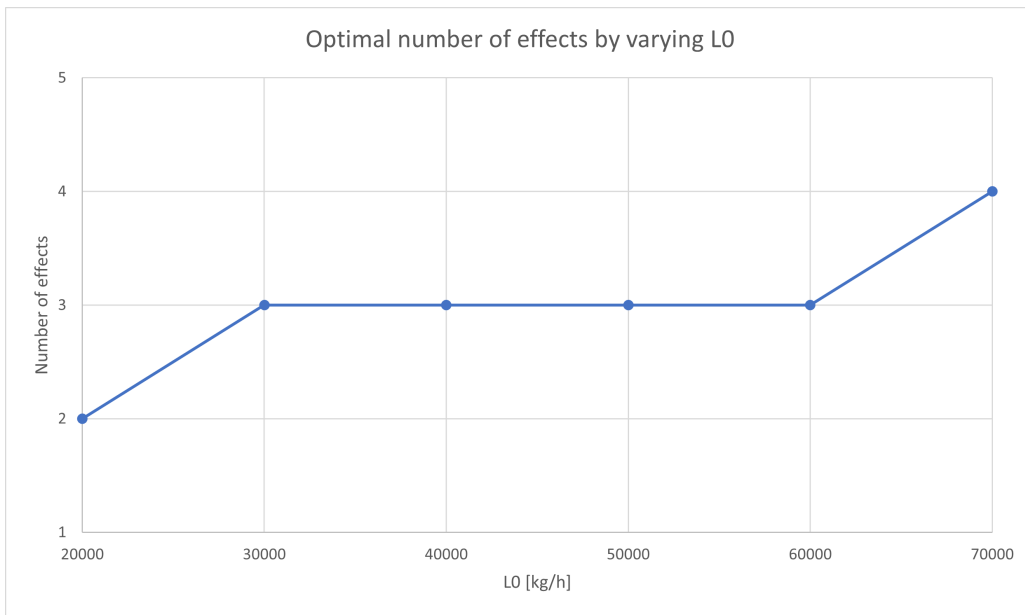


Figure 10: Effect of feed flow rate (L_0) on the optimal number of effects.

3.3.2 Variation in Evaporation Target

The second part of the sensitivity analysis explores the effect of varying the evaporation target, defined as the total amount of water to be removed from the feed stream, V_{tot} . In this analysis, the inlet flow rate L_0 is kept constant, while V_{tot} is adjusted to represent different final concentration levels. To ensure consistency, the evaporation target is expressed as a percentage of the inlet flow rate. The evaluated scenarios include evaporation targets equal to 40%, 50%, 60%, 70%, 75%, 85%, 90%, 95%, and 99% of L_0 .

Each case corresponds to a different level of product concentration, with higher percentages representing more intensive evaporation. The total cost was evaluated across configurations from one to five effects. The results, illustrated in Figure 11, show that:

- With an evaporation target of 40% of L_0 , a **two-effect** configuration is optimal.
- With a target of 99%, a **four-effect** configuration becomes preferable.
- In all other cases, the **three-effect** configuration remains optimal.

However, the 99% and 95% scenarios lack physical significance, as the initial feed L_0 contains only 94% water. These cases were analyzed solely to theoretically identify the point at which evaporation would reach a level that shifts the optimal configuration from three to four effects.

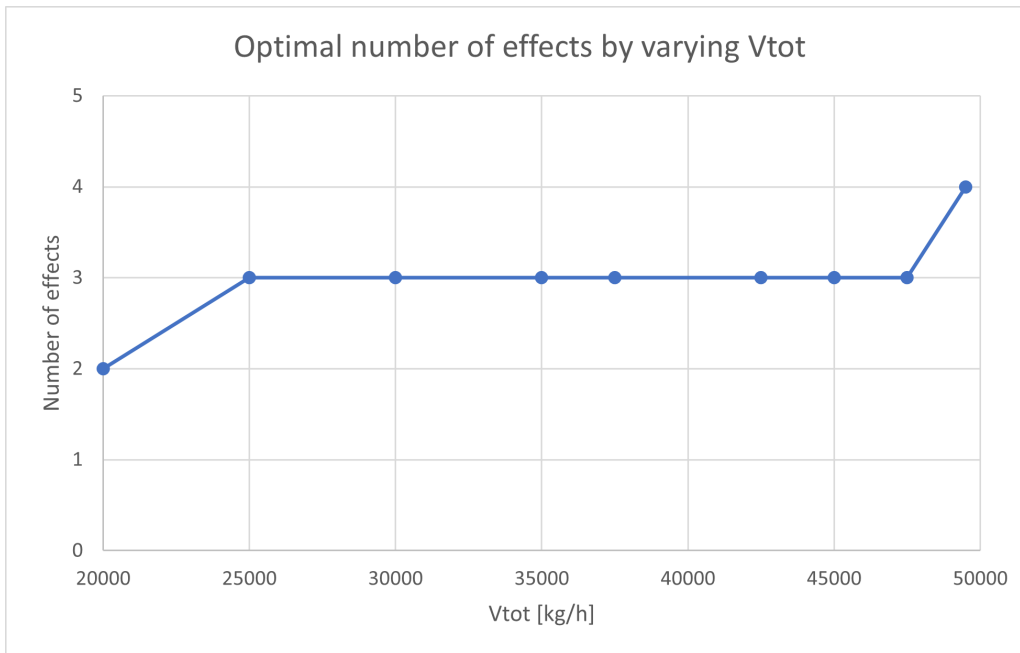


Figure 11: Effect of Evaporation Target (V_{tot}) on the optimal number of effects.

3.4. The Digital Twin

Following the thermodynamic and economic analysis of the evaporator system, the digital twin is implemented in AVEVA Dynamic Simulation based on the optimal three-effect configuration identified during the cost optimization phase. As described in Subsection 2.5 — *The Digital Twin* — of Section 2 — *Materials and Methods*, the model is designed to replicate both the physical dynamics of the process and the architecture of its control strategy.

The simulation directly reflects the mass and energy balances previously defined and it is expected to reproduce the theoretical design results. The primary objective is to verify internal consistency across the system, ensuring that flow paths, control logic, pressure gradients, and heat transfer mechanisms are accurately implemented across the three evaporator effects.

To evaluate the system’s dynamic behavior under realistic operating conditions, both start-up and shutdown scenarios are simulated. These include a detailed analysis of temperature, pressure and liquid level trends within the three effects.

To better visualize the results, the numerical outputs from the simulation are processed by exporting data as CSV files. These datasets are then imported in Excel to remove eventual unfeasible points. Three graphs for each scenarios are then produced, each illustrating the time evolution of a specific variable in the three evaporators (blue, orange, and green lines respectively), highlighting the response of the feed-forward control system. This visual representation allows for an immediate comparison between the dynamic model and the expected process behavior, providing a basis for validating the implemented control strategy.

3.4.1 Start-up Scenario Results

This section presents the temporal trends in temperature, pressure and level variations within the three evaporators during the startup scenario. The analysis highlights the dynamic behavior and evolution of these key process variables as the system transitions from initial conditions to steady operation.

Figure 12 illustrates the dynamic temperature evolution in each of the three evaporator effects throughout the start-up sequence. The behavior reflects the sequential thermal activation of the system and the effectiveness of the controlled heating strategy implemented in DynSim.

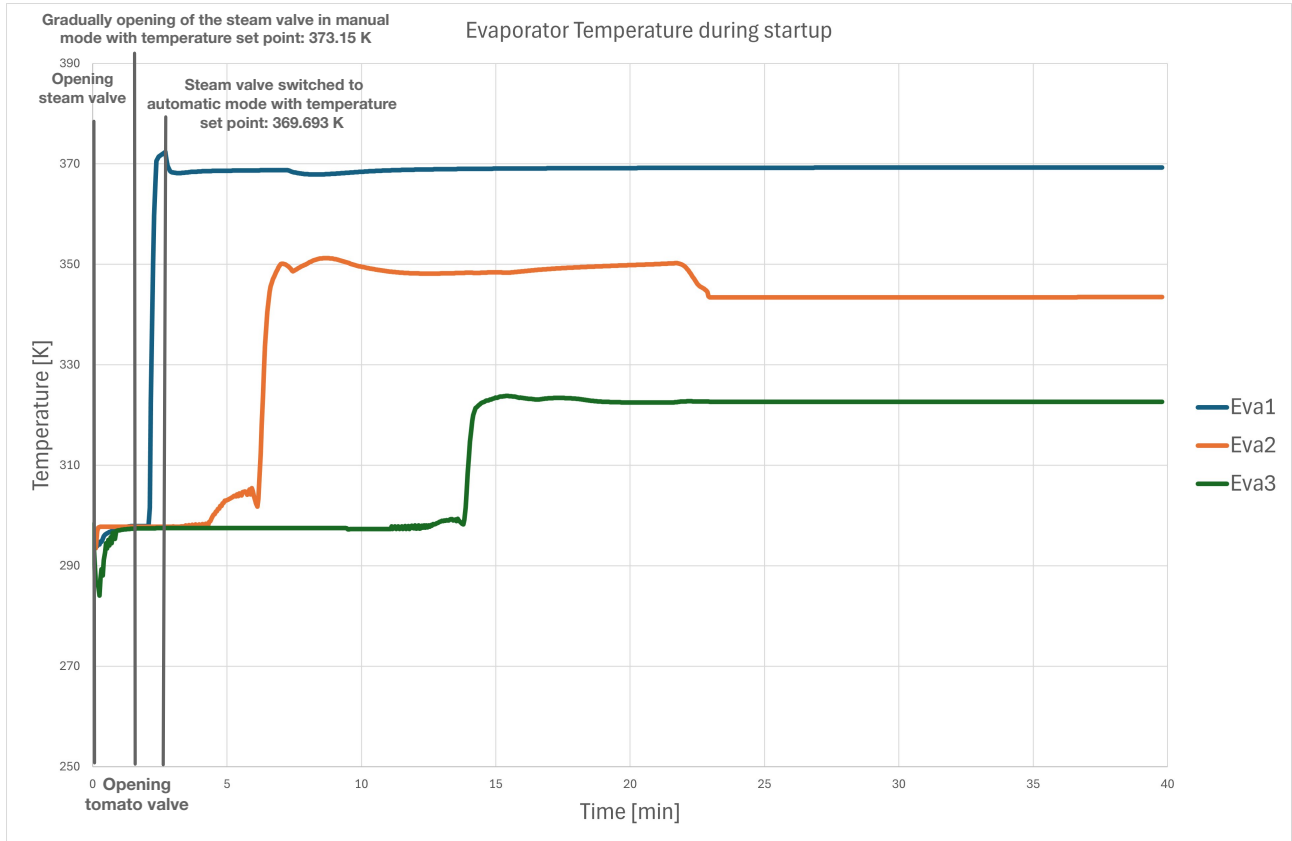


Figure 12: Dynamic evolution of temperatures in the three evaporators during the start-up phase

Immediately following the initial opening of the steam valve, noticeable fluctuations are observed in the temperature profiles. These are attributed to the absence of feed within the system, leading to unstable thermal conditions.

Once the tomato feed valve (XV1) is opened and the steam controller (PID2) begins operating in manual mode, with a setpoint of 373.15 K (100 °C), the temperature in the first evaporator rises rapidly. As soon as this temperature reaches the desired level (371.15 K/ 98°C), the steam controller switches to automatic mode, with the setpoint adjusted to 369.693 K (96.243 °C). This gradual transition ensures a controlled and uniform heating of the first effect, minimizing thermal stress on equipment. Around minute 4, the first evaporator reaches thermal equilibrium, stabilizing at approximately 369 K (96 °C). From this point, its temperature remains nearly constant, indicating that steady-state thermal conditions have been achieved.

The second evaporator begins to heat up more significantly around minute 6, corresponding to the moment it starts receiving hot liquid from the first effect. After an initial transient with some fluctuations, the temperature stabilizes at around 345 K (72 °C).

In contrast, the third evaporator remains near ambient temperature during the initial phase of start-up. Its temperature begins to rise only at around minute 14, once product transfer from the second effect begins. Shortly after, by minute 15, its temperature stabilizes at approximately 322 K (49 °C).

Overall, the system reaches full thermal steady-state conditions across all three effects within the first 15 minutes of operation.

Figure 13 shows the dynamic evolution of pressure within the three evaporator effects during startup, highlighting the sequential pressurization of the system.

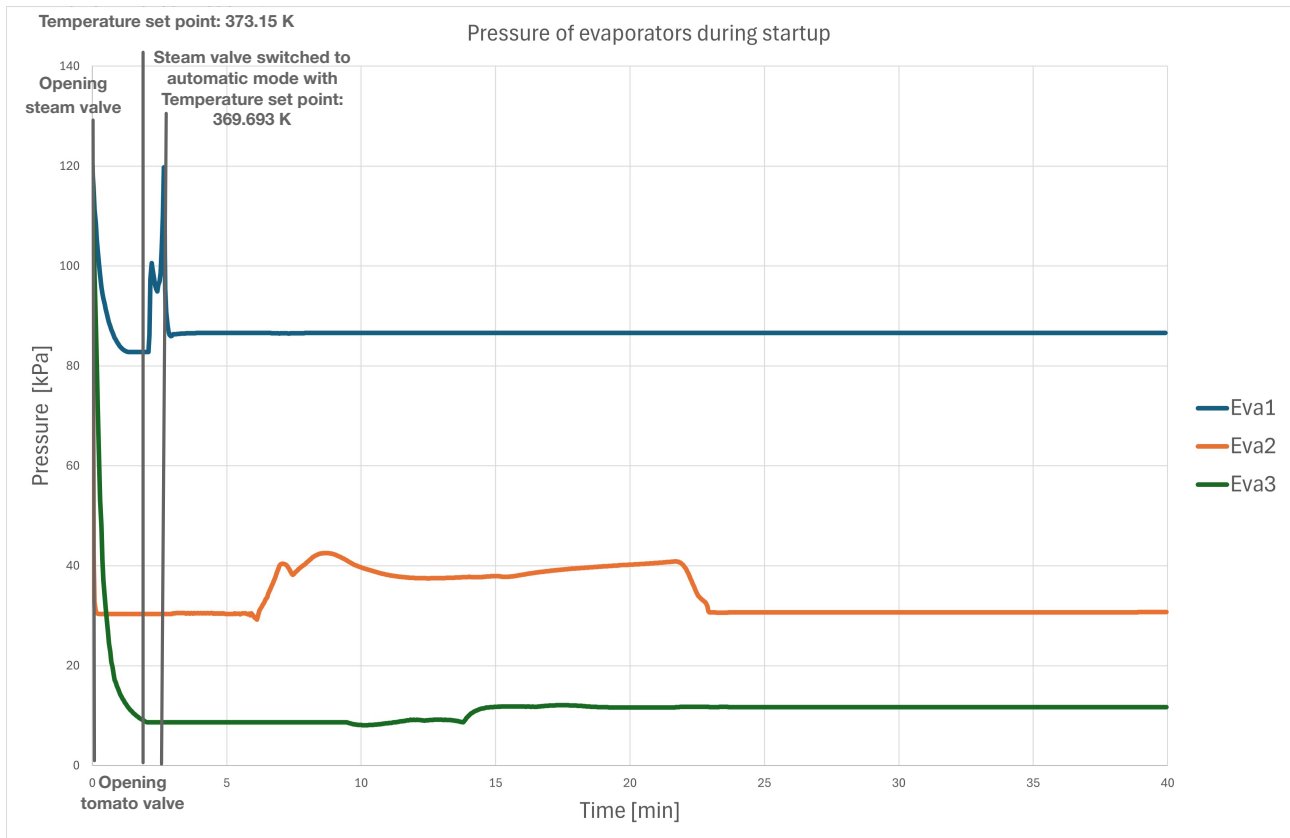


Figure 13: Dynamic evolution of pressures in the three evaporators during the start-up phase

At the beginning of the procedure, the steam valve (XV2) is opened gradually in manual mode, with a temperature setpoint of 373.15 K. This results in a smooth decrease, with some initial fluctuations, in the pressure of the first effect, indicating the start of heat transfer and vapor generation. Simultaneously, the pressure in the second and third effects begins to decrease as well. Throughout the entire transient phase, all pressures remain below atmospheric pressure (under vacuum). This vacuum operation is essential to allow evaporation at reduced temperatures, which is critical for preserving thermally sensitive compounds such as lycopene and pectin. Operating under lower pressures reduces the boiling point of the product in each stage, thereby protecting its quality while improving energy efficiency.

As expected, the pressure decreases progressively from the first to the third effect, reflecting the design of the system where vapor from one effect is reused as the heating medium for the next. This pressure gradient is fundamental to the thermodynamic operation of the evaporator and for ensuring the natural flow of liquid stream from one effect to the next.

The switch to automatic steam control at a lower temperature setpoint (approximately 369.7 K) results in pressure stabilization.

A closer look at the pressure profile reveals a slight increase in the second effect approximately from minute 6 to 22, consistent with the temperature trend of this effect. This behavior is attributed to the initial imbalance between vapor generation in the first effect and condensation in the second. As steam is introduced and the first effect begins producing vapor, the second effect momentarily accumulates vapor more rapidly than it can fully condense or transfer to the third stage, causing a transient pressure and temperature rise. Once thermal equilibrium is approached and inter-effect heat exchange stabilizes, the pressure in the second effect settles at its expected steady-state value.

Figure 14 shows the dynamic behavior of the liquid levels in the three evaporator effects during the start-up sequence. The graph illustrates how the levels evolve over time as the system transitions from an initial state to steady operation.

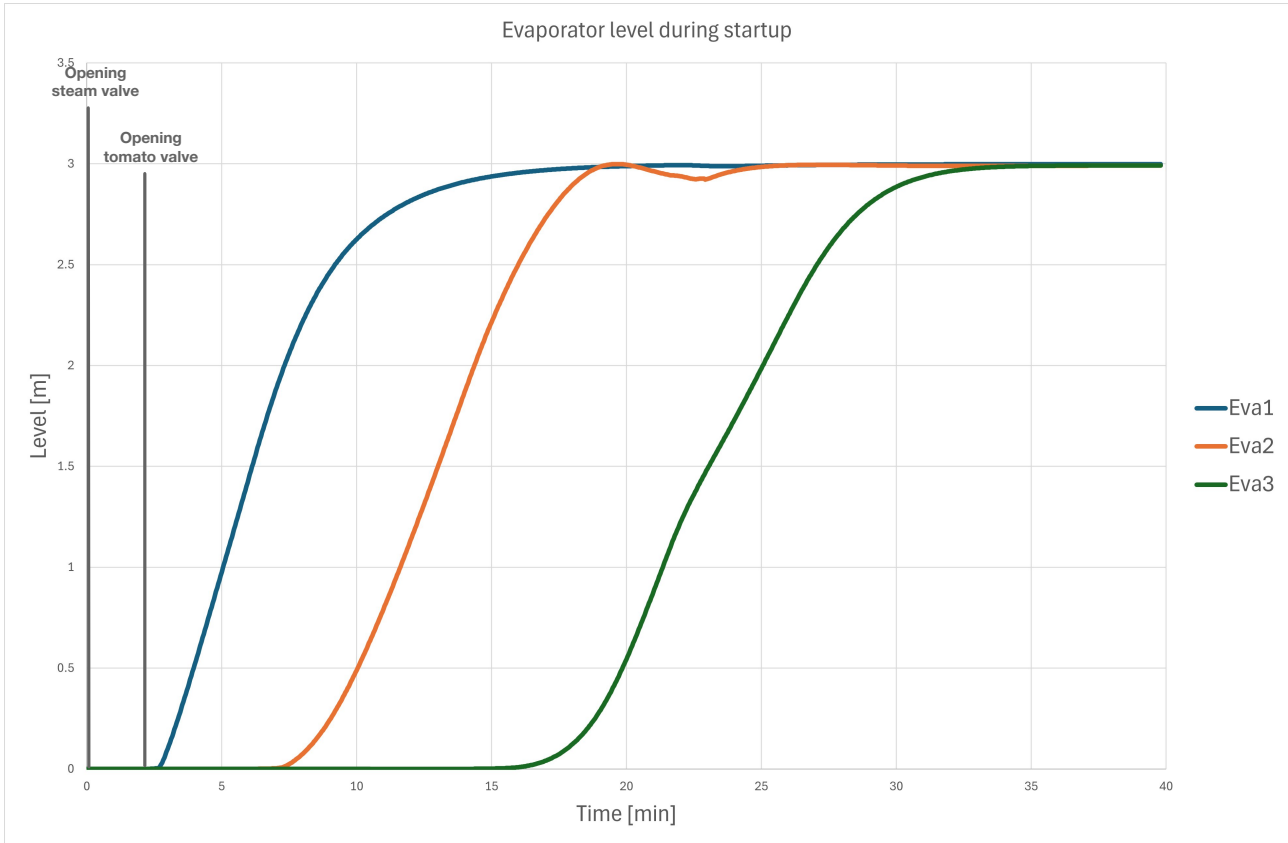


Figure 14: Dynamic evolution of liquid levels in the three evaporators during the start-up phase

Following the initial opening of the steam valve, the system begins to heat up while all liquid inlet valves remain closed. During this phase, the liquid levels remain zero across all evaporators, as no feed is introduced. After the completion of the pre-heating phase, the tomato juice valve is opened, initiating a controlled feed into the first evaporator.

As the feed enters, the liquid level in the first effect rises rapidly, followed by a delayed but sequential increase in the levels of the second and third effects.

Accordingly to what the temperature and pressure trends have revealed, the second evaporator liquid level shows a little fluctuation around minute 20, when the third evaporator starts receiving liquid from the second one. At this specific point, the second effect drain more liquid than what it receives, but it rapidly stabilizes after a few minutes.

This progressive activation reflects the cascading feed-forward configuration of the system, where the overflow from each evaporator becomes the input for the next stage. All three levels stabilize as the system reaches steady-state conditions at three meters in half an hour.

In summary, the start-up procedure successfully brings the evaporation system to stable operating conditions within approximately 30 minutes, in terms of temperature/pressures profiles and liquid levels across the three effects. However, while internal conditions stabilize relatively quickly, the fresh steam supply to the system, denoted as V_0 , reaches its steady-state flow rate of approximately 11,500 kg/h only after about nine hours. This slow approach to steady state reflects the dynamic interaction between the control loops and the system's thermal inertia: as the system nears the setpoint, the rate of change naturally decreases.

3.4.2 Shut-down Scenario Results

This section analyzes the dynamic response of the evaporation system during the shutdown phase, with particular focus on the evolution of temperature, pressure and liquid levels in each evaporator effect. The simulation reproduces a controlled drain-down procedure initiated from the steady-state conditions, established after nine hours of continuous operation.

The shutdown sequence is designed to safely bring the system to a fully deactivated state by isolating the feed and steam inputs and sequentially emptying the vessels. Monitoring the transient trends of key process variables ensures that safe conditions are achieved for maintenance activities or subsequent restart operations, while minimizing the risk of thermal or mechanical stress.

Figure 15 illustrates the dynamic temperature behavior of the three-effect evaporator system during the shut-down procedure. The sequence involves the complete closure of the steam and tomato feed valves (XV2 and XV1, respectively), along with the full opening of the bottom outlet valves of each evaporator (XV4, XV5, XV7) to initiate draining.

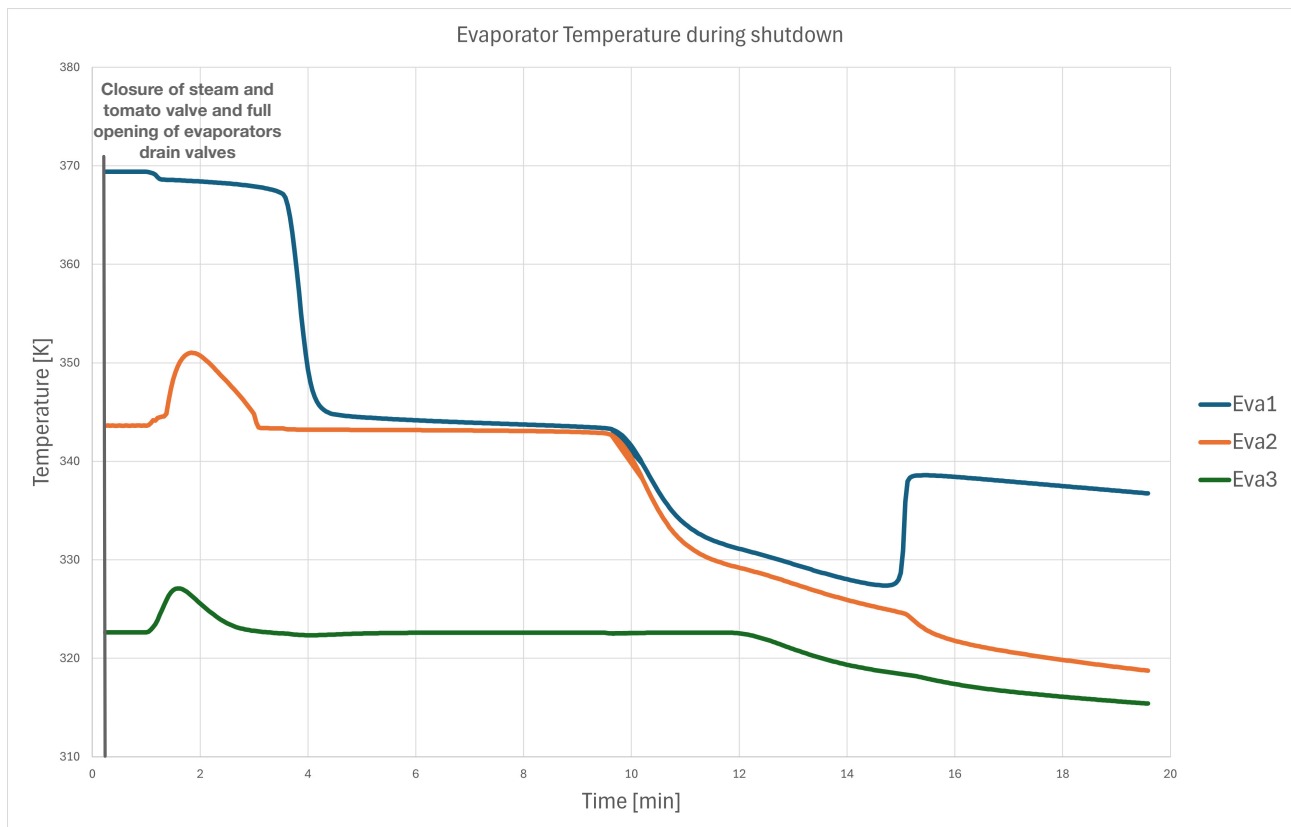


Figure 15: Dynamic evolution of temperatures in the three evaporators during the shut-down phase

Following the adjustment of the valves, the temperature in the first effect begins to decrease gradually due to the closing of steam input. Around minute 4, the temperature drops to approximately 340 K (67 °C). A pattern emerges where the temperature decreases smoothly at first, followed by a more abrupt drop, reaching below 330 K (57 °C) by minute 5. Interestingly, after this point, the temperature rises sharply to about 339 K (66 °C) and then stabilizes, likely due to residual steam accumulation or local recirculation effects before the vessel is fully emptied.

The second effect shows a different trend. Its temperature remains relatively stable, around its steady-state value of 345 K (72 °C), up to minute 10, coinciding with the moment the liquid level inside the vessel reaches zero. A minor fluctuation occurs around minute 2, marked by a slight increase, which may be attributed to local thermal imbalance as the feed from the first effect stops. After the vessel is emptied, the temperature gradually decreases, falling to approximately 320 K (47 °C) by the end of the shutdown.

The third effect exhibits a similar behavior to the second. Its temperature remains nearly constant until minute 12, which corresponds to the time when the liquid content is fully drained. Following this, the temperature begins a smooth decline, eventually dropping below 320 K (47 °C), consistent with the absence of incoming hot liquid and the progressive cooling of the vessel.

Figure 16 illustrates the dynamic evolution of pressures during the shutdown phase.

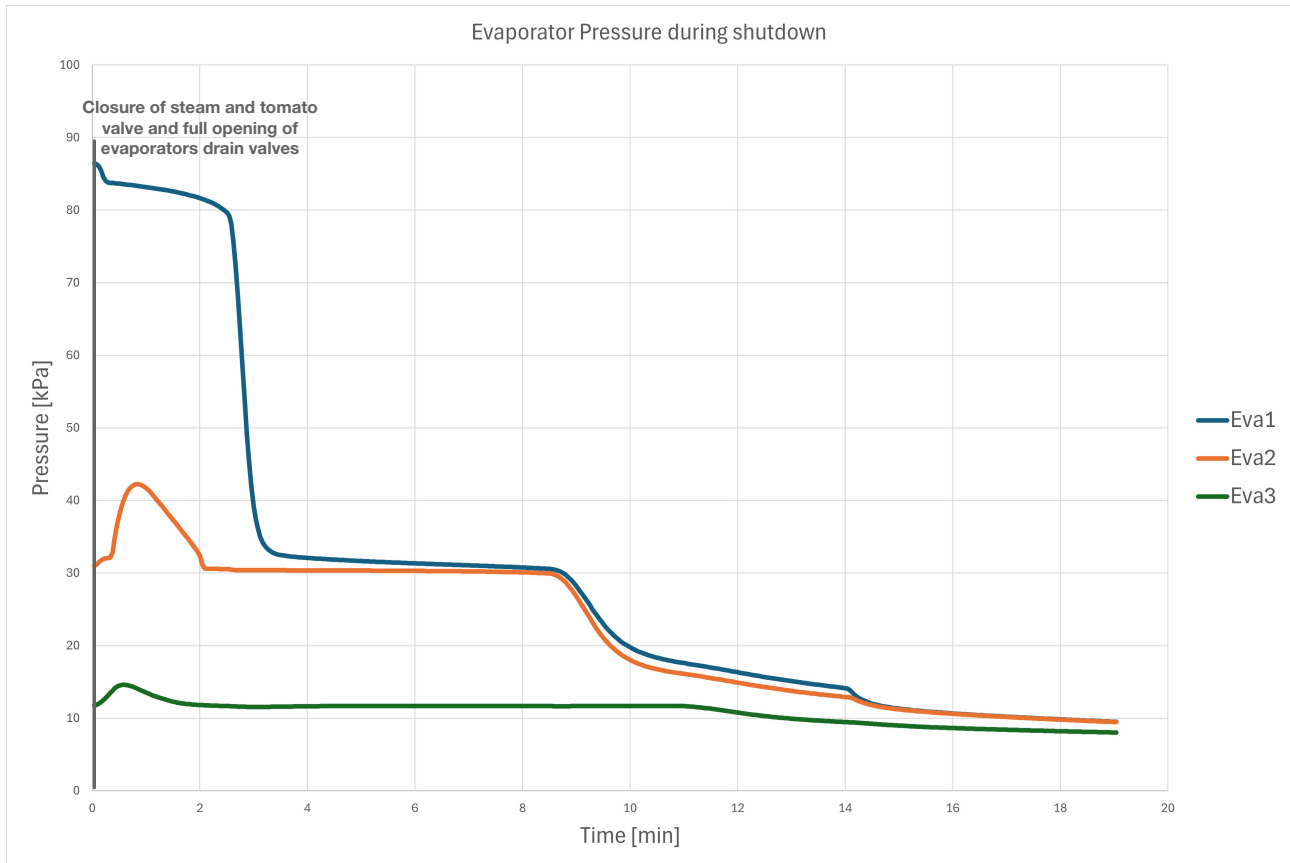


Figure 16: Dynamic evolution of pressures in the three evaporators during the shut-down phase

The shutdown phase is initiated by the simultaneous closure of both the steam and tomato feed valves (XV2, XV1), along with the full opening of the drain valves of all evaporators (XV4, XV5, XV7). Following the steam cut-off, a sharp decrease in pressure is observed across all three effects. The loss of thermal input influences vapor generation almost immediately, and without continuous feed or heating, the internal pressure begins to drop as vapor condenses and the remaining liquid is drained. As during startup, all pressure values remain within the vacuum range throughout the shutdown, reinforcing the system's design for sub-atmospheric operation to avoid excessive boiling temperatures.

The pressure decline is particularly pronounced in the first effect, consistent with its temperature profile during the shut-down. As shown in the temperature trends during the draining phase also the pressure exhibits a brief plateau. Once the evaporators are empty they gradually depressurize. Notably, the pressure in the second and third effect exhibit an initial increase attributed to the draining of the first effect, which causes a small liquid accumulation in the other drums.

Ultimately, pressures in all three effects converge toward a low steady-state vacuum level, indicating the removal of both product and vapor from the system.

Figure 17 shows the dynamic evolution of liquid levels in the three evaporator effects during the shutdown procedure. Approximately one minute after the procedure is initiated, the liquid levels begin to respond, departing from their steady-state values.

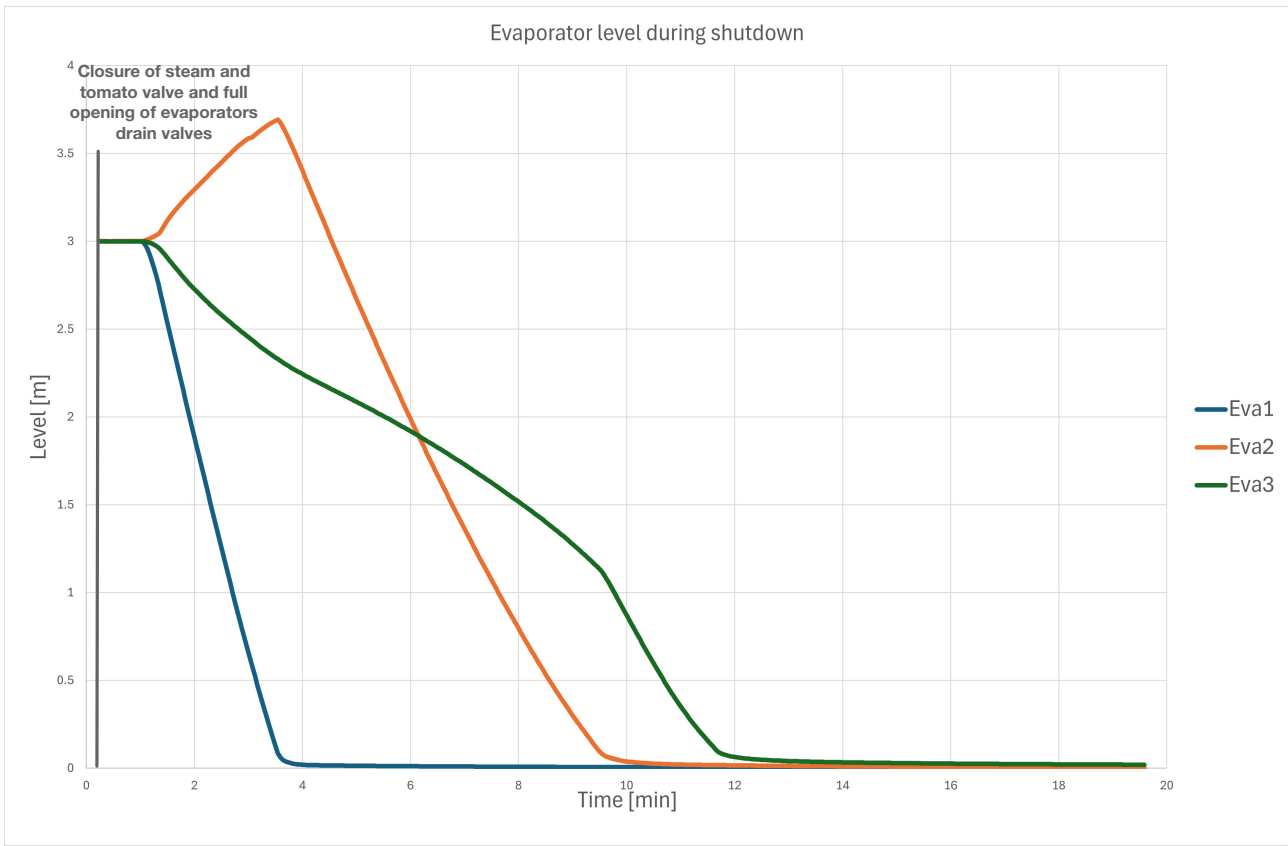


Figure 17: Dynamic evolution of liquid levels in the three evaporators during the shut-down phase

The first effect exhibits a rapid and continuous decrease in liquid level, reaching zero by minute 4. This quick discharge reflects the immediate impact of isolating the steam supply and fully opening the outlet valve, combined with the absence of incoming feed.

The second effect displays a more complex behavior. Initially, its level increases slightly, surpassing 3.5 meters, indicating it is receiving more liquid than what it is able to drain. This brief rise is likely due to the residual outflow from the first effect, which continues for a short period even after the feed is stopped. Around minute 4, coinciding with the complete drainage of the first effect, the second effect’s level begins to decline. The decrease occurs more gradually compared to the first effect and reaches zero by minute 10.

The third effect follows a two-phase drainage pattern. From the beginning of the shutdown until minute 10, the liquid level decreases smoothly, indicating a slower draining rate. After minute 10, when the second effect is fully empty, the decline becomes more pronounced and rapid, leading to full drainage by minute 12.

The shutdown simulation demonstrates that the evaporator system safely transitions from steady-state operation to a fully deactivated, drained condition in a controlled manner. Complete drainage is achieved within approximately 12 to 16 minutes across the effects, with each vessel reaching zero level without oscillations or hydraulic transients. These results ensures that evaporator vessels are left in a safe state, suitable for maintenance or subsequent startup operations.

4. Conclusions and Further Development

This work focuses on the design, economic optimization, and dynamic simulation of a forward-feed multiple-effect evaporation system for tomato paste production. Starting from a 50,000kg/h, 5°Brix feed and targeting a concentrate of about 30 °Brix, the analysis compares configurations ranging from one to five effects and develops a Digital Twin of the optimal configuration in DynSim to assess start-up and shut-down operations.

Among one to five effects, the three-effect configuration minimizes the total cost under the study assumptions (Table 11). The corresponding fresh-steam demand V_0 is 11,534.34 kg/h and the total evaporated water V_{tot} is 40,955.76 kg/h, giving a steam economy of 3.55. Effect-by-effect balances produce an outlet concentration close to 28% w/w solids, with progressively lower temperatures and pressures along the effects, consistent with vacuum operation and quality preservation.

The Digital Twin reproduces the expected thermodynamic behavior and control interactions. During start-up, effects reach thermal steady conditions within roughly 15 min and liquid levels settle within about 30 min, while the fresh-steam flow asymptotically approaches its nominal value. The shut-down script achieves safe vessel drainage in about 12–16 min without oscillations or hydraulic upsets, confirming a robust sequence.

The three-effect forward-feed arrangement achieves a favorable CapEx/OpEx trade-off while preserving heat-sensitive compounds thanks to the temperature cascade under vacuum. The Digital Twin is a valuable engineering tool: it reduces trial-and-error during start-up and shut-down, supports controller tuning, and provides a safe environment to test “what-if” scenarios such as changes in throughput or set-points, ultimately helping to save energy, enhance operability, and maintain product quality.

Future work should address the reduction of start-up time, as the current scenario shows that the fresh steam flow requires several hours to reach its nominal steady-state value despite internal temperatures and levels stabilizing earlier. Possible improvements include refining control strategies, adjusting valve characteristics, or introducing preheating systems to achieve faster thermal stabilization.

The Digital Twin currently represents only the evaporation section. Extending the model to upstream (pretreatment, juice extraction) and downstream (sterilization, packaging) units would enable an integrated simulation of the entire plant, allowing the evaluation of inter-unit dynamics and the impact of operational changes on the complete process.

Once validated with industrial data, the Digital Twin could be used as a plant-wide optimization and decision-support tool. It could improve energy efficiency by identifying opportunities for steam and heat recovery, for example through the system described in the section 2.4 — *Packaging heat exchanger* — of 2 — *Results*, adjust operating set-points in response to changes in feed flow rate or composition, and simulate “what-if” scenarios, such as equipment failures or process modifications, without interrupting production. It could also serve as a realistic training platform, allowing operators to practice start-up, shut-down, and emergency procedures in a safe environment.

Future developments could also involve the integration of Artificial Intelligence (AI) and Machine Learning (ML) within the Digital Twin framework. Building on the validated model and reconciled data, this integration could follow a staged approach: (i) physics-informed soft sensors to estimate unmeasured states such as effective heat-transfer coefficients or fouling resistance; (ii) predictive maintenance and anomaly detection using temporal models trained on historical operating data to forecast maintenance needs and detect deviations; (iii) energy-aware supervisory optimization, where learned surrogate models of the evaporation system could be embedded within model predictive control (MPC) or safe reinforcement learning (RL) algorithms to optimize start-up trajectories and steam consumption; and (iv) transfer learning across recipes or production lines to accelerate adaptation while monitoring performance indicators such as start-up time and steam use. This roadmap leverages the existing Digital Twin and requires only incremental instrumentation and logging to implement advanced predictive and adaptive functionalities [6].

References

- [1] Emadaldin Elfatih M. Abdurrahman and Giovanna Ferrari. Digital twin applications in the food industry: A review. *Frontiers in Sustainable Food Systems*, 9:1538375, 2025.
- [2] Ahmed A. Al-Kafrawy, Yehia Abd El-Razik Heikal, Ihab S. Ashoush, and Samar M. Mahdy. Effect of processing on the characterization of hot-break triple-concentrated tomato paste. *Egyptian Journal of Chemistry*, 2022.
- [3] Belkis Avalo and Alfredo Varela. Modeling and simulation of a triple effect evaporator for the concentration of natural juices. *Revista Técnica de la Facultad de Ingeniería, Universidad del Zulia*, 31(2):151–158, 2008. Accessed: 2025-06-30.
- [4] Sheryl A. Barringer. Tomato products. In Arun Tapre and Girish Joshi, editors, *Processing Vegetables: Science and Technology*, pages 139–158. Technomic Publishing Co., 2003.
- [5] Sheryl A. Barringer. Concentration of tomato juice and paste. In Y.H. Hui, editor, *Handbook of Vegetable Preservation and Processing*, pages 423–438. CRC Press, 2004.
- [6] Marcello Maria Bozzini, Marco Menegon, Alberto di Loreto, Gaia Lunari, Silvia Serena Mariani, Mattia Vallerio, Laura Piazza, and Flavio Manenti. Towards smarter food manufacturing through digital twins. *eff aidic*, page 24, 2025.
- [7] François-Xavier Branthôme. Tomato products: Navigating global markets, consumer insights, and product dynamics, 2023. Accessed: 2025-08-04.
- [8] François-Xavier Branthôme. Global exports of tomato paste, updated may 14, 2024, 2024. Accessed: 2025-08-04.
- [9] ChemicalBook. Acido folico (cas no. 59-30-3) – proprietà chimiche e dati di sicurezza. https://www.chemicalbook.com/ChemicalProductProperty_EN_CB5100903.htm, 2025. Ultimo aggiornamento: 27 giugno 2025, accesso: 2 luglio 2025.
- [10] ChemicalBook. Vitamin a (cas no. 68-26-8) – chemical product & property data. https://www.chemicalbook.com/ChemicalProductProperty_EN_CB8194893.htm, 2025. Accessed: 2025-07-02.
- [11] Morning Star Company. 2024 post-season global tomato crop update, 2024. Accessed: 2025-08-04.
- [12] Corporate Finance Institute. Understanding capex vs opex, 2023.
- [13] Farnaz Ganjeizadeh, Nikita Gupta, Anamika Burile, and Helen Zong. Optimization of multiple effect evaporation system via modelling and simulation. *Journal of Food Engineering*, 278:109926, 2020.
- [14] Wilbur A. Gould. *Tomato Production, Processing and Technology*. CTI Publications, Inc., Baltimore, Maryland, 1983.
- [15] Don W. Green and Robert H. Perry. *Perry’s Chemical Engineers’ Handbook*. McGraw-Hill, New York, 8th edition, 2008.
- [16] Investopedia. Capital expenditure (capex), 2023.
- [17] Investopedia. Operating expense (opex), 2023.
- [18] Seid Mahdi Jafari, Esra Çapanoglu, and Asli Can Karaca, editors. *Evaporation Technology in Food Processing*. Elsevier, Amsterdam, 2024.
- [19] S. Jha et al. Vacuum evaporation to preserve quality and nutrients in tomato products. *Journal of Food Engineering*, 2021.
- [20] S.A. Klein and G.F. Nellis. *Thermodynamics*. Cambridge University Press, Cambridge, 2008. Appendix B: Property Tables for Water.
- [21] Eunmi Koh, Suthawan Charoenprasert, and Alyson E Mitchell. Effects of industrial tomato paste processing on ascorbic acid, flavonoids and carotenoids and their stability over one-year storage. *Journal of the Science of Food and Agriculture*, 91(1):151–161, 2011.

- [22] Flavio Manenti. Slides on process design of evaporators, 2024. Lecture slides, Politecnico di Milano.
- [23] Ali Motamedzadegan and Hoda Shahiri Tabarestani. Tomato production, processing, and nutrition. In *Food Processing: Strategies for Quality Assessment*, chapter 36. Wiley-Blackwell, 2018. Department affiliations: Sari Agricultural Sciences and Natural Resources University; Gorgan University of Agricultural Sciences and Natural Resources.
- [24] Mutti SpA. 2022 tomato processing season: Mutti happy with the quality of tomatoes despite rising energy costs and drought, 2022. Accessed via internal document.
- [25] Emmanuel O. Oloruntoba, Bamidele A. Olunlade, and Folahan I. Ibitoye. Effects of input variables on the conversion of 5 ton/h processed tomato juice in a triple-effect evaporator. *British Journal of Applied Science & Technology*, 17(4):1–12, 2016.
- [26] Nicola Onger. Studio di un impianto per la produzione di concentrato di pomodoro, 2021.
- [27] R. Simpson, S. Almonacid, D. López, and A. Abakarov. Optimum design and operating conditions of multiple effect evaporators: Tomato paste. *Journal of Food Engineering*, 102(2):136–144, 2008.
- [28] Rafael M. Soares, Maurício M. Câmara, Thiago Feital, and José Carlos Pinto. Digital twin for monitoring of industrial multi-effect evaporation. *Processes*, 7(8):531, 2019.
- [29] Z. Sogut, N. Ilten, and Z. Oktay. Energetic and exergetic performance evaluation of the quadruple-effect evaporator unit in tomato paste production. *Energy*, 35(4):1536–1544, 2010.
- [30] Z. Sogut, N. Ilten, and Z. Oktay. Energetic and exergetic performance evaluation of the quadruple-effect evaporator unit in tomato paste production. *Energy*, 44:578–584, 2012.
- [31] Beli R. Thakur, Rakesh K. Singh, and Avtar K. Handa. Chemistry and uses of pectin — a review. *Journal Name*, 2025. Review article.
- [32] Gavin Towler and Ray Sinnott. *Chemical Engineering Design: Principles, Practice and Economics of Plant and Process Design*. Butterworth-Heinemann, Oxford, UK, 3rd edition, 2022.
- [33] A. Trifirò, M. Giacometti, and D. Mastrocola. Effect of air incorporation on lycopene degradation during tomato paste processing. *Industria Alimentari*, 37(370):456–460, 1998.
- [34] Richard Turton, Richard C. Bailie, Wallace B. Whiting, Joseph A. Shaeiwitz, and Debangsu Bhattacharyya. *Analysis, Synthesis, and Design of Chemical Processes*. Prentice Hall, Upper Saddle River, NJ, 4th edition, 2012.
- [35] USDA-AMS. United states standards for grades of canned tomatoes, 1983. United States Department of Agriculture, Agricultural Marketing Service.
- [36] Wikipedia contributors. Niacina — wikipedia, l’enciclopedia libera. <https://it.wikipedia.org/wiki/Niacina>, 2025. Ultima modifica: 2 luglio 2025, accesso: 2 luglio 2025.
- [37] Wikipedia contributors. Riboflavina — wikipedia, l’enciclopedia libera. <https://it.wikipedia.org/wiki/Riboflavina>, 2025. Ultima modifica: 2 luglio 2025, accesso: 2 luglio 2025.
- [38] Wikipedia contributors. Tiamina — wikipedia, l’enciclopedia libera. <https://it.wikipedia.org/wiki/Tiamina>, 2025. Ultima modifica: 2 luglio 2025, accesso: 2 luglio 2025.
- [39] World Processing Tomato Council. Production, 2022. Accessed: 2025-09-05.
- [40] Qin Xu, Irma Adyatni, and Bradly Reuhs. Effect of processing methods on the quality of tomato products. *Department of Food Science, Purdue University*, 2018. Whistler Center for Carbohydrate Research.
- [41] YASA Ltd. Multiple effect evaporator: Forward feed, backward feed & parallel feed for multi effect evaporation, 2023.

5. Abstract in Lingua Italiana

La tesi affronta lo studio della progettazione, dell'ottimizzazione e della simulazione dinamica di un sistema di evaporazione equicorrente multi-stadio, finalizzato alla produzione di concentrato di pomodoro. Questo prodotto, ottenuto portando il succo da 5 a 30 °Brix, rappresenta un ingrediente di grande rilevanza a livello mondiale, non solo per il suo largo impiego nell'industria alimentare, ma anche per il contenuto di composti bioattivi come licopene, pectina e vitamina C, la cui conservazione dipende fortemente dalle condizioni di processo. L'analisi combina il design del sistema con una valutazione dei costi, al fine di individuare il numero ottimale di effetti nel processo di evaporazione. Inoltre, integra la tecnologia dei Digital Twin nell'ambito dell'Industria 4.0, per studiarne il comportamento dinamico. Grazie ad una valutazione economica comparativa su configurazioni da uno a cinque effetti, considerando investimenti iniziali, costi operativi e spesa complessiva lungo l'intero ciclo di vita dell'impianto, emerge che la configurazione a tre effetti in equicorrente rappresenta la soluzione più conveniente in termini di costo totale. Il Digital Twin della configurazione ottimale, sviluppato con il software AVEVA Dynamic Simulation, riproduce fedelmente la dinamica del sistema e consente di simulare le fasi di avviamento e arresto dell'impianto. Il modello mostra un controllo di processo affidabile, una buona stabilità durante l'avviamento e un drenaggio sicuro degli evaporatori nella fase di arresto. In conclusione, il lavoro mette in evidenza come i Digital Twin possano contribuire a una migliore comprensione dei processi, a una maggiore sicurezza operativa e a un supporto più efficace alle decisioni nell'industria alimentare, promuovendo allo stesso tempo sostenibilità e competitività.

6. Acknowledgements

We would like to express our sincere gratitude to our advisor, Prof. Flavio Manenti, for his trust and for giving us the opportunity to carry out our thesis under his guidance. A special thanks goes to our co-advisor, Marcello Maria Bozzini, for his constant support, patience, availability, and guidance throughout this journey.

We are truly grateful for the opportunity they offered us to take part in the Engineering Future Food (EFF) 2025 congress in Bologna, giving us our first chance to grow and challenge ourselves beyond the academic environment.

Finally, we would like to thank our families for their care and encouragement, always standing by us with patience, understanding, and love. Their presence has been a constant source of strength and motivation, and their support has been essential in reaching this milestone.